

Research Paper

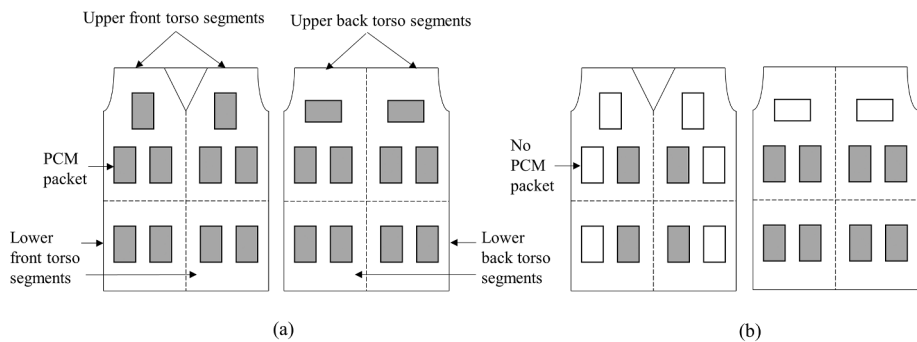
Significance of PCM arrangement in cooling vest for enhancing comfort at varied working periods and climates: Modeling and experimentation

Mariam Itani^a, Nesreen Ghaddar^{b,*}, Kamel Ghali^b, Djamel Ouahrani^a, Beatrice Khater^c^a Department of Architecture and Urban Planning, College of Engineering, Qatar University, P.O. Box 2713, Doha, Qatar^b Mechanical Engineering Department, American University of Beirut, P.O. Box 11-0236, Beirut 1107-2020, Lebanon^c Department of Family Medicine, American University of Beirut Medical Center, Beirut, Lebanon

HIGHLIGHTS

- Significance of PCM arrangement in cooling vest to enhance comfort was studied.
- Experiments on six male subjects validated the versatility of a bio-heat and fabric-PCM model.
- Case studies were done by varying ambient conditions, working period and PCM coverage area.
- Optimal comfort was attained with full back followed by upper front coverage over lower front.
- Higher coverage area showed less differences between optimal and worst case at longer durations.

GRAPHICAL ABSTRACT



Schematics showing: (a) Cooling vest upper and lower front torso segments fully covered with PCM packets and (b) Cooling vest with partial coverage on front and back torso segments

ARTICLE INFO

Keywords:

Phase change material
Cooling vest modeling
Bio-heat modeling
Core and skin temperatures
Thermal comfort and sensation

ABSTRACT

Personal cooling vests that incorporate phase change material (PCM) have been utilized to improve thermal sensation of people working outdoors in different fields (firefighting, construction, military, police, etc.). In this study, an integrated fabric-PCM and bio-heat model was validated through human subject testing to determine the extent to which it could detect thermal and comfort responses when varying the arrangement of a fixed number of PCM packets in the cooling vest. The modeling approach was utilized for given PCM melting temperature to determine the number of packets needed and their optimal arrangement at moderate (35 °C) and hot (40 °C) environments for 45, 60 and 90 min working durations. The findings showed that when full coverage of the torso is not needed, optimal arrangements were those having full back coverage with the remaining packets on the upper front. Lower front cooling did not show significant improvement in comfort over upper front cooling. That effect was more evident when lower front PCM packets were used at the 40 °C hot environment. As the working duration increased, less differences were detected in skin temperatures and comfort between the optimal and worst cases since a higher PCM coverage area was necessary.

* Corresponding author.

E-mail address: farah@aub.edu.lb (N. Ghaddar).<https://doi.org/10.1016/j.applthermaleng.2018.09.057>

Received 16 August 2017; Received in revised form 4 July 2018; Accepted 11 September 2018

Available online 14 September 2018

1359-4311/ © 2018 Elsevier Ltd. All rights reserved.

Nomenclature

<i>A</i>	area (m ²)
<i>Age</i>	age of the participant (years)
<i>B</i>	back segment of the torso
<i>BWL</i>	body weight loss (g)
<i>C</i>	specific heat (J/kg·K)
<i>d</i>	gap width (m)
<i>e</i>	thickness (m)
<i>ECG</i>	electrocardiogram
<i>Exp.</i>	experimental results
<i>g</i>	gravitational acceleration (m/s ²)
<i>F</i>	front segment of the torso
<i>h_{ad}</i>	heat of adsorption (J/kg)
<i>h_c</i>	convective heat transfer (W/m ² ·K)
<i>h_f</i>	heat transfer coefficients (kg/m ² ·kPa·s)
<i>h_{fg}</i>	heat of evaporation (J/kg)
<i>h_m</i>	mass transfer coefficient (kg/m ² ·kPa·s)
<i>h_{sf}</i>	latent heat of fusion (J/kg)
<i>IRTT</i>	infrared tympanic thermometer
<i>ISO</i>	International Organization for Standardization
<i>l</i>	width of PCM packet (m)
<i>LF</i>	lower front torso segment
<i>m</i>	mass (kg)
<i>m_a</i>	microclimate air mass flow rate (kg/s)
<i>m_{sw}</i>	sweat mass flow rate per unit area (kg/m ² ·s)
<i>MET</i>	Metabolic Equivalent for Task
<i>n</i>	number of PCM packets
<i>No vest</i>	no vest is worn by the participant
<i>P</i>	vapor pressure (kPa)
<i>PE</i>	perceived exertion
<i>PCM</i>	phase change material
<i>r</i>	radius (m)
<i>R_d</i>	dry thermal resistance of the fabric (m ² ·K/W)
<i>R_e</i>	evaporative resistance of the fabric (m ² ·kPa/W)
<i>R</i>	fabric regain
<i>Sim.</i>	simulation results
<i>t</i>	time (s)
<i>T</i>	temperature (°C)
<i>T_B</i>	back skin temperature (°C)
<i>T_F</i>	front skin temperature (°C)
<i>TC</i>	thermal comfort
<i>TTS</i>	torso thermal sensation
<i>UF</i>	upper front torso segment
<i>w</i>	humidity ratio (kg _w /kg _{air})
<i>WBGT</i>	wet bulb globe temperature (°C)

<i>2UF-OLF-10B</i>	2 PCM packets placed on UF torso, 0 on LF torso and 10 on back torso
<i>4UF-OLF-10B</i>	4 PCM packets placed on UF torso, 0 on LF torso and 10 on back torso
<i>2UF-2LF-10B</i>	2 PCM packets placed on UF torso, 2 on LF torso and 10 on back torso
<i>0UF-4LF-10B</i>	0 PCM packets placed on UF torso, 4 on LF torso and 10 on back torso
<i>4UF-2LF-8B</i>	4 PCM packets placed on UF torso, 2 on LF torso and 8 on back torso
<i>4UF-4LF-6B</i>	4 PCM packets placed on UF torso, 4 on LF torso and 6 on back torso
<i>6UF-4LF-4B</i>	6 PCM packets placed on UF torso, 4 on LF torso and 4 on back torso

Greek symbols

<i>α</i>	fraction of melted PCM
<i>β</i>	volumetric thermal expansion (°C ⁻¹)
<i>Δ</i>	change
<i>λ</i>	condensation rate (kg/m ² ·s)
<i>ν</i>	kinematic viscosity of air (m ² /s)
<i>ρ</i>	density (kg/m ³)
<i>Ψ</i>	condensation coefficient

Subscripts

<i>a</i>	microclimate air
<i>air</i>	macroclimate air
<i>avg</i>	average
<i>cr</i>	core
<i>dp</i>	dew point
<i>env</i>	environment
<i>i</i>	body segment index
<i>if</i>	inner fabric
<i>in</i>	inner
<i>j</i>	PCM packet index
<i>mean</i>	mean
<i>of</i>	outer fabric
<i>out</i>	outer
<i>o,w,avg</i>	difference between optimal and worst cases averaged over time
<i>o,w,end</i>	difference between optimal and worst cases at the end of working period
<i>sat</i>	saturated
<i>skin</i>	skin layer

1. Introduction

People working outdoors in different fields (firefighting, military, police, construction, etc.) are subjected to warm or hot conditions that place them under the risk of heat stress. In addition, global warming and its effects on the outdoor climate increases the risk of heat stress [1]. Heat stress can cause productivity loss of workers and measures would be needed to avoid such occurrences [2]. Wearing a cooling vest incorporating different phase change material (PCM) is one of the methods suggested for decreasing heat stress and improving labor endurance of outdoor workers [3–6]. Cooling vests fully covered on the inner side with PCM packets targeted the human trunk region which was reported to be an influential body region on improving thermal comfort when locally cooled in warm environment [7–10].

Different working durations exist depending on the task type and whether it requires light or heavy activity and if it is performed in warm or hot ambient conditions. For example, a working duration in

moderate conditions might be as short as 30 min with firefighters wearing protective clothing [11] and could increase to two hours with moderate activity levels [12]. Previous experimental and modeling studies showed that cooling vests with full PCM coverage can reduce local torso skin temperatures and improve human thermal comfort [13,14]. However, these studies did not take into consideration that a short working duration might require less PCM coverage area before complete melting.

The complete PCM packet melting depends on the temperature difference between the human skin and the PCM, the packet melting temperature and its heat of fusion, the working duration, and the ambient conditions [4,5,15]. Previous studies, that conducted experiments using PCM cooling vests, did not focus on the amount of PCM needed for total melting of the packets. House et al. [13] conducted tests on human subjects who did exercise for 45 min and rested for another 45 min while wearing PCM vests of different melting temperatures at the hot environment of 40 °C. Their results showed that total melting

did not happen in the 30 °C PCM packets by end of the 90-min exposure. In the work of Gao et al. [4], total melting did not happen of the 28 °C PCM packets after the human subjects cycled for 20 min in ambient conditions of 20 °C and then walked for 24 min on a treadmill in very hot condition of 55 °C. Gao et al. [14] also performed human subject experiments, where the participants sat at a workstation in a moderate environment at 34 °C for 60 min while wearing the vest. The vest was fully covered with packets having a melting point of 21 °C and a total PCM weight of 1,785 g. Their results showed that the vest was able to provide about 3 °C temperature drop in torso skin temperature and improve overall and torso thermal sensations, without complete melting of the packets.

Hence, for short working durations, depending on the PCM properties and ambient conditions, fully filling the cooling vest with PCM packets may not be necessary. Moreover, the advantage brought by the PCM cooling vest comes at the expense of added weight on the human body and the hindrance of water vapor transmission, which may affect the vest performance. In such a situation, it is desirable to reduce the weight of the vest by using the minimum amount of packets that would result in complete melting by the end of the work duration, while effectively cooling the body.

Cotter and Taylor [8] studied local thermo-sensitivities for the different body regions (face, upper and lower limbs and torso; chest, abdomen and lower back). They concluded that the torso, after the face, had higher thermo-sensitivity for sudomotor control and was relatively more sensitive to cooling than other body parts. The regional sensitivity to a cold stimulus was examined by Stevens [16] who reported that the back followed by the chest and abdomen were the most sensitive regions. Moreover, Zhang et al. [7] developed empirical correlations to predict comfort and sensation based on extensive experiments on 109 human subjects. They reported that when the body was warm, cooling the chest (upper front, UF) would provide higher comfort than cooling the pelvis (lower front, LF). Cooling only the back was shown to

improve overall comfort compared to cooling only the front at environment temperature of 28 °C using 8 PCM packets [17]. It is of interest to determine the minimum number of packets (or PCM coverage area) that would be needed to avoid carrying extra weight for a given activity level at different working durations and at moderate and hot environmental conditions. Then, when the working conditions do not require fully filling the vest with PCMs, the question would be about the best order of placement of the packets on the torso segments; UF, LF, and back, that would show the highest improvement in thermal comfort.

To answer the questions on establishing minimum number of PCM models and their placement on the torso to improve comfort, it is important to use a multi-segmental bio-heat model that can accurately predict human thermal responses as well as comfort and sensation in transient and non-uniform conditions [6,7,18]. Recently, Itani et al. [6] utilized an integrated bio-heat and fabric-PCM model to predict optimal PCM arrangement in the cooling vest recommended for outdoor workers for a working period of two hours in a moderate environment [12]. At the ambient condition of 32 °C, it was concluded that placing 8 packets with a melting point of 28 °C on the back segment was the optimal case. However, in the study [6], the focus was for a fixed number of PCM packets and for moderate ambient conditions by performing simulations using a model validated with published experimental data. Moreover, previous studies did not recommend the order of torso segments that should be first covered with PCM packets in case total torso coverage was not needed. As a matter of fact, physiological models of the human body are approximate with inherent empirical relations, accordingly, there is a need to ensure that the model findings are also observed by humans wearing the vests. This requires validation of model via testing on active participants in controlled environmental conditions.

The integrated bio-heat of Karaki et al. [18] and fabric-PCM model of Itani et al. [6,19] was validated with tests on thermal manikin but

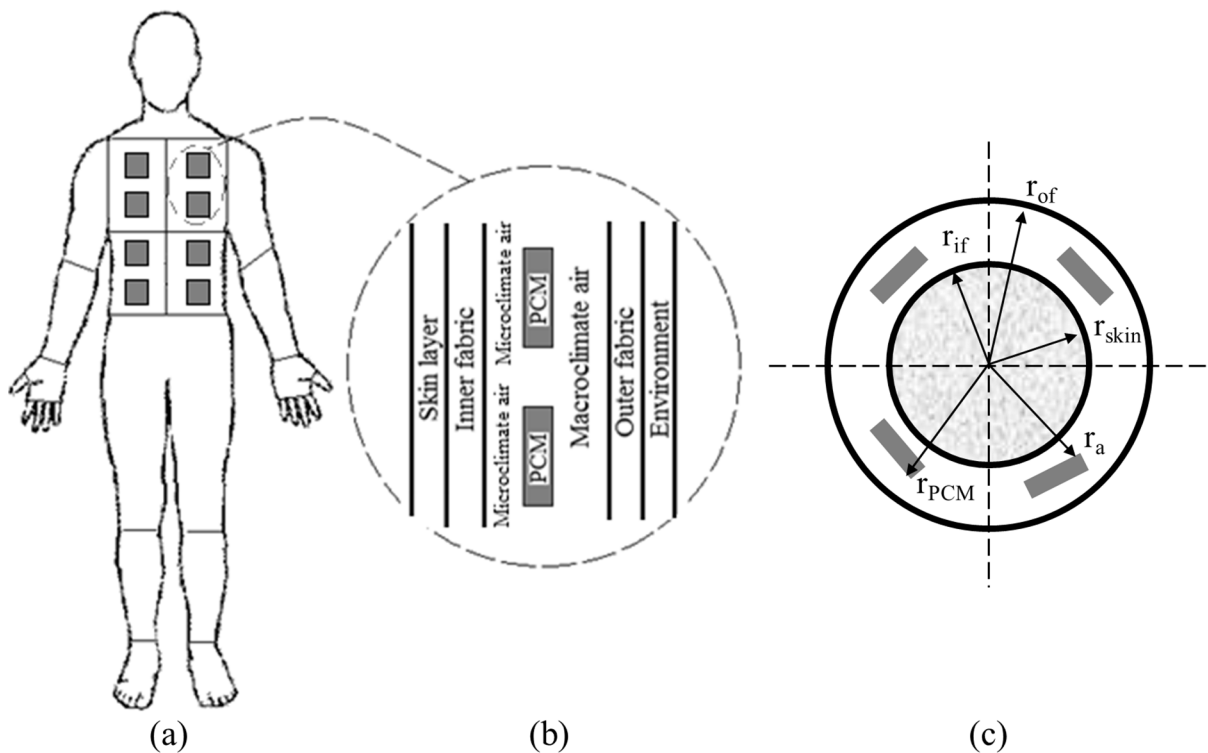


Fig. 1. Schematics showing (a) a human body with the torso covered with PCM packets (b) a side view of the PCM packet in a cooling vest sandwiched between the human skin and environment and (c) a top view of the vest with PCM packet covering different segments and the radii of the corresponding layers.

has not been tested on human subjects wearing the cooling vest. In this work, the integrated fabric-PCM and bio-heat model will be validated through human subject testing to determine the extent to which the model is capable of detecting physiological responses and comfort sensations when varying the arrangement of a fixed number of PCM packets in the vest. In addition, the experiments will identify the placement of PCM packets that provides optimal comfort, through unequal number of PCM packets placed on the torso segments; UF, LF and back. Different comfort scales exist in literature including, but not limited to, the McGinnis scale [20], Predicted Mean Vote [21] and Zhang et al. [7] comfort scale. Zhang et al. [7] comfort and sensation scale was used in this study since it can predict local and overall comfort and sensation in transient and steady state conditions and it can be easily integrated with the bio-heat model. Finally, the validated model is utilized to find the minimum number and associated optimal arrangement of PCM packets needed to achieve best comfort for different typical working durations at environments of 35 °C and 40 °C while ensuring the complete melting of PCM by the end of the working period.

2. Mathematical modeling

In this study, a versatile integrated multi-segmental bio-heat [18], a fabric-PCM model [6,19] and a comfort and sensation model [7] were utilized to predict physiological, thermal and subjective responses of humans wearing cooling vests with optimal placement of a certain number of packets on human torso. The focus in this study targeted the use of unequal PCM coverage on three segments; UF, LF and back, in accordance with Zhang et al. [7] comfort model. The placement of packets affects the regional skin temperatures which in turn influences the thermal comfort of the wearer [8,19]. After validating the model via human subject testing, the modeling approach was applied to a number of case studies at different working durations and environmental conditions to find the minimum number of packets for comfort and their optimal placement on the torso segments.

2.1. Integrated bio-heat and comfort and sensation model

The integrated model constituted of a multi-node segmental transient bio-heat model of Karaki et al. [18] and a comfort and sensation model of Zhang et al. [7]. The bio-heat model divided the human body into 31 segments and its torso into 8 segments (2 upper front, 2 lower front, 2 upper back and 2 lower back) as shown in the schematic in Fig. 1(a). The area of the upper torso segments (0.402 m²) was larger than that of the lower ones (0.246 m²). Each torso segment has a skin node, thus, the bio-heat model was sensitive to angular variations in the torso environment. In addition, the model took into consideration the effect of extremely hot conditions exceeding 39 °C [22] and the effect of the carried weight [23] on the metabolism by increasing it by a factor equal to 2.7% for each additional kg in carried weight. Detailed description of the utilized bio-heat model can be found in previous studies [18,24]. However, the bio-heat model required the following main input parameters:

- Initial thermal state of the human.
- Clothed and unclothed segments and the clothing properties (dry and evaporative resistances, density and thickness).
- Metabolic rate of the human.
- Ambient temperature and relative humidity.

The bio-heat model was integrated with the model of Zhang et al. [7], which includes empirical correlations and makes use of the core and skin temperatures and their rate of change to find transient thermal sensation and comfort. The subjective scales vary from -4 (very cold or very uncomfortable) to +4 (very hot or very comfortable).

2.2. Fabric-PCM model

The cooling vest (SWEDE cooling vest) [25] is made up of an inner and outer fabric layer that are exposed to the human skin and environment, respectively, as shown in a side view of a part of the cooling vest in Fig. 1(b). The vest has 20 pockets that can hold 20 PCM packets covering the torso. The fabric-PCM model divided the vest into four layers; inner fabric layer near the skin, microclimate air layer behind each PCM packet, macroclimate air layer in front and in between the packets and the outer fabric layer exposed to the ambient. The inner fabric layer was in contact with the skin on one hand and exposed to the microclimate region behind each PCM packet and the macroclimate region on the other. The PCM packet was closer to the inner fabric layer due to the Velcro fasteners and thus, a thin microclimate region was present. The PCM packet would directly affect the microclimate air region and would allow vertical buoyancy motion to happen in the thin microclimate layer [26]. Thus, the inner fabric, having a specific dry thermal resistance, exchanges heat with the skin via conduction. In addition, the inner fabric exchanges heat with the macroclimate and microclimate air, respectively, via convection. The macroclimate air layer in front of the PCM packets and in between the packets was considered to be lumped for each torso segment, as shown in Fig. 1(b). The PCM packets, prior to wearing the vest, would be in a solid state and are affected by the heat gained from the hot environment and the microclimate air near the skin. In addition, the fabric-PCM model accounted for the increase in the resistance brought by the dissimilarity in the areas of the vest layers [27]. This dissimilarity was due to the cylindrical geometry and is represented by a ratio of the radii shown in the top view of the PCM vest in Fig. 1(c).

The model of the fabric-PCM considered mass and energy balances for each fabric and air layer as well as an energy balance for the PCM packet and its melted fraction. The different mass balances considered horizontal water vapor exchange between the skin and inner fabric, and between the inner fabric and the air layers along with moisture loss by condensation. The different energy balances considered heat exchange between the skin and inner fabric and between the inner fabric and air layers as well as heat loss by condensation. Moreover, an energy balance was used to predict the PCM temperature during the non-melting phase and the melted fraction during melting of the PCM packet. During melting, the PCM temperature is constant and is equal to its melting temperature. The PCM packets exchanged heat with the micro and macro climate air layers and would be affected if condensation happens at the relatively cool surface of the PCM. Condensation causes the release of latent heat that would decrease the performance of the PCM packet. The different mass and energy equations for the vest layers and PCM packet are presented below:

Energy balance of inner fabric layer:

$$\underbrace{\rho_{if} * A_{if,i} * e_{if} * C_{if} * \frac{dT_{if,i}}{dt}}_{\text{transient storage term}} - \underbrace{\rho_{if} * A_{if,i} * e_{if} * h_{ad} * \frac{dR_{if,i}}{dt}}_{\text{heat due to absorption of water vapor}} = \underbrace{\frac{T_{skin,i} - T_{if,i}}{\frac{R_{d,if}}{2} * \frac{r_{if}}{r_{skin}}} * A_{if,i}}_{\text{conductive heat transfer from skin to inner fabric}} - \underbrace{\frac{T_{if,i} - T_{ai,j}}{\left(\frac{R_{d,if}}{2} + \frac{1}{2 * h_{f,in}}\right)} * \sum_{j=1}^n A_{PCMj}}_{\text{convective heat transfer from inner fabric to microclimate air}} - \underbrace{\frac{T_{if,i} - T_{air,i}}{\left(\frac{R_{d,if}}{2} + \frac{1}{2 * h_{f,in}}\right)} * \left(A_{if,i} - \sum_{j=1}^n A_{PCMj}\right)}_{\text{convective heat transfer from inner fabric to macroclimate air}} \tag{1}$$

Mass balance of inner fabric layer:

$$\underbrace{\rho_{if} * A_{if} * e_{if} * \frac{dR_{if,i}}{dt}}_{\text{transient storage term}} = \underbrace{\frac{P_{skin,i} - P_{if,i}}{\left(\frac{R_{e,if} * h_{fg}}{2}\right) * \frac{r_{if}}{r_{skin}}} * A_{if,i}}_{\text{moisture transfer by diffusion from skin to inner fabric}} - \underbrace{\frac{P_{if,i} - P_{air,i}}{\left(\frac{R_{e,if} * h_{fg}}{2} + \frac{1}{2 * h_{m,in}}\right)} * \left(A_{if,i} - \sum_{j=1}^n A_{PCMi,j}\right)}_{\text{moisture transfer by convection from inner fabric to macroclimate air}} - \underbrace{\frac{P_{if,i} - P_{ai,j}}{\left(\frac{R_{e,if} * h_{fg}}{2} + \frac{1}{2 * h_{m,in}}\right)} * \sum_{j=1}^n A_{PCMi,j}}_{\text{moisture transfer by convection from inner fabric to microclimate air}} \quad (2)$$

Energy balance of outer fabric layer:

$$\underbrace{\rho_{of} * A_{of} * e_{of} * C_{of} * \frac{dT_{of,i}}{dt}}_{\text{transient storage term}} - \underbrace{\rho_{of} * A_{of} * e_{of} * h_{ad} * \frac{dR_{of,i}}{dt}}_{\text{heat due to absorption of water vapor}} = \underbrace{\frac{T_{env} - T_{of,i}}{\left(\frac{R_{d,of}}{2} + \frac{1}{2 * h_{f,out}}\right)} * A_{of,i}}_{\text{convective heat transfer from outer fabric to environment}} + \underbrace{\frac{T_{air,i} - T_{of,i}}{\left(\frac{R_{d,of}}{2} + \frac{1}{2 * h_{f,in}}\right) * \frac{r_{of}}{r_{if}}} * A_{of,i}}_{\text{convective heat transfer from macroclimate air to outer fabric}} \quad (3)$$

Mass balance of outer fabric layer:

$$\underbrace{\rho_{of} * A_{of} * e_{of} * \frac{dR_{of,i}}{dt}}_{\text{transient storage term}} = \underbrace{\frac{P_{env} - P_{of,i}}{\left(\frac{R_{e,of} * h_{fg}}{2} + \frac{1}{2 * h_{m,out}}\right)} * A_{of,i}}_{\text{moisture transfer by diffusion from outer fabric to environment}} + \underbrace{\frac{P_{air,i} - P_{of,i}}{\left(\frac{R_{e,of} * h_{fg}}{2} + \frac{1}{2 * h_{m,in}}\right) * \frac{r_{of}}{r_{if}}} * A_{of,i}}_{\text{moisture transfer by convection from macroclimate air to outer fabric}} \quad (4)$$

In Eqs. (1) through (4), the indices *if*, *of*, *air*, *a*, *skin*, *env* and *j* indicate the inner fabric, outer fabric, macroclimate air, microclimate air, skin, environment and an index for the PCM packet number, respectively. The symbols *e*, *ρ*, *C*, *R_e*, *R_d*, *h_m*, *h_f* and *h_{ad}* represent the fabric thickness, density, specific heat, evaporative resistance, dry thermal resistance, mass transfer coefficient, heat transfer coefficient and heat of adsorption, respectively. The heat transfer coefficient in the micro and macro climate air layers was taken from the experimental data on internal heat transfer coefficients with air gaps between 5 and 10 mm in the study of Danielsson [28]. The symbols *A*, *r*, *P*, *h_{fg}*, *n* and *i* represent the area, radius, vapor pressure, heat of evaporation, number of packets, and an index for the body segment, respectively.

The PCM temperature, *T_{PCMi,j}*, can be predicted during non-melting using Eq. (5), in which the symbol *Ψ* considers the effect of condensation. In addition, *a_{i,j}*, the PCM melted fraction, can be obtained during melting using Eq. (6), where *Ψ* is set to unity in the presence of condensation, otherwise, *Ψ* is zero, as shown in Eq. (7). Condensation would take place on the PCM packet surface only if it is below the macroclimate air dew point temperature, *T_{dp,air,b}* or the microclimate one, *T_{dp,a,i,j}*.

PCM temperature during non-melting phase:

$$\underbrace{m_{PCMi,j} * C_{PCM} * \left(\frac{dT_{PCMi}}{dt}\right)}_{\text{transient storage term}} = \underbrace{\frac{T_{ai,j} - T_{PCMi,j}}{\left(\frac{1}{h_c}\right) * \frac{r_{PCM}}{r_{if}}} * A_{PCMi,j}}_{\text{convective heat transfer from microclimate air to PCM}} + \underbrace{\frac{T_{air,i} - T_{PCMi,j}}{\left(\frac{1}{h_c}\right)} * A_{PCMi,j}}_{\text{convective heat transfer from PCM to macroclimate air}} + \underbrace{\Psi * (\lambda_{ai,j} + \lambda_{air,i}) * h_{fg} * A_{PCMi,j}}_{\text{heat released by condensation of water vapor on PCM surface}} \quad (5)$$

PCM melted fraction during melting:

$$\underbrace{m_{PCMi,j} * h_{sf} * \left(\frac{d\alpha_{PCMi}}{dt}\right)}_{\text{transient storage term}} = \underbrace{\frac{T_{ai,j} - T_{PCMi,j}}{\left(\frac{1}{h_c}\right) * \frac{r_{PCM}}{r_{if}}} * A_{PCMi,j}}_{\text{convective heat transfer from microclimate air to PCM}} + \underbrace{\frac{T_{air,i} - T_{PCMi,j}}{\left(\frac{1}{h_c}\right)} * A_{PCMi,j}}_{\text{convective heat transfer from PCM to macroclimate air}} + \underbrace{\Psi * (\lambda_{ai,j} + \lambda_{air,i}) * h_{fg} * A_{PCMi,j}}_{\text{heat released by condensation of water vapor on PCM surface}} \quad (6)$$

$$\text{where } \Psi = \begin{cases} 1 & \text{if } T_{PCMi,j} < T_{dp,a,i,j} \text{ or } T_{dp,air,i} \\ 0 & \text{else} \end{cases} \quad (7)$$

The symbols *m*, *h_{sf}*, and *h_c* represent the PCM mass, PCM latent heat of fusion and the convective heat transfer coefficient, respectively. The symbols *λ_{ai,j}* and *λ_{air,i}* represent the segmental condensation rates of the micro and macro climate air, respectively.

The mass flow rate of the microclimate air, *ṁ_{ai,j}*, is obtained using Eq. (8) with the assumption of Poiseuille flow [26]:

$$\dot{m}_{ai,j} = \rho_{air} g \beta \frac{T_{air,i} - T_{ai,j}}{12\nu} (d)^3 l \quad (8)$$

The symbols *d*, *β*, *g*, *ν* and *l* represent the gap width, the thermal expansion coefficient of air, the gravitational acceleration, the kinematic viscosity of air and the PCM packet width, respectively.

Mass and energy balances are also utilized to find the segmental microclimate air humidity ratio, *w_{ai,j}*, condensation rate, *λ_{ai,j}*, and temperature, *T_{ai,j}*, along with the macroclimate air temperature, *T_{air,b}*, humidity ratio, *w_{air,b}* and condensation rate, *λ_{air,b}* as follows:

Mass balance of microclimate air:

$$\underbrace{\rho_{air} * d * \left(\frac{dw_{ai}}{dt}\right)}_{\text{transient storage term}} = \underbrace{\frac{P_{if,i} - P_{ai,j}}{\sum \left(\frac{R_{e,if} * h_{fg}}{2} + \frac{1}{2 * h_{m,in}}\right) * \frac{r_{if}}{r_{if}}}}_{\text{moisture transfer by convection from inner fabric to microclimate air}} - \underbrace{\dot{m}_{ai,j} * (w_{air,i} - w_{ai,j}) * \frac{1}{d * l}}_{\text{moisture transfer due to microclimate air ventilation}} - \underbrace{\Psi * \lambda_{ai,j}}_{\text{moisture transfer due to water vapor condensation}} \quad (9)$$

Energy balance of microclimate air:

$$\underbrace{\rho_{air} * d * A_{PCMi,j} * C_{air} * \left(\frac{dT_{ai}}{dt}\right)}_{\text{transient storage term}} = \underbrace{\frac{T_{if,i} - T_{ai,j}}{\left(\frac{1}{h_c}\right) * \frac{r_{ai}}{r_{if}}} * A_{PCMi,j}}_{\text{convective heat transfer from inner fabric to microclimate air}} + \underbrace{\frac{T_{PCMi,j} - T_{ai,j}}{\frac{1}{h_c}} * A_{PCMi,j}}_{\text{convective heat transfer from PCM to microclimate air}} + \underbrace{\dot{m}_{ai,j} * C_{air} * (T_{air,i} - T_{ai,j})}_{\text{heat transfer by microclimate air ventilation}} - \underbrace{\Psi * \lambda_{ai,j} * h_{fg} * A_{PCMi,j}}_{\text{heat released by condensation of water vapor}} \quad (10)$$

Mass balance of macroclimate air:

$$\underbrace{\rho_{air} * e_{air} * \frac{dw_{air,i}}{dt}}_{\text{transient storage term}} = \underbrace{\left(\frac{P_{of,i} - P_{air,i}}{\left(\frac{R_{e,if} * h_{fg}}{2} + \frac{1}{2 * h_{m,in}} \right)} \right)}_{\text{moisture transfer by convection from macroclimate air to outer fabric}} + \underbrace{- \Psi * \lambda_{air,i}}_{\text{moisture transfer due to water vapor condensation}} + \underbrace{\sum_{j=1}^n \dot{m}_{ai,j} (w_{ai,j} - w_{air,i}) * \frac{1}{d * l}}_{\text{moisture transfer due to microclimate air ventilation}} + \underbrace{\left(\frac{P_{if,i} - P_{air,i}}{\left(\frac{R_{e,if} * h_{fg}}{2} + \frac{1}{2 * h_{m,in}} \right)} \right) * \left(A_{if,i} - \sum_{j=1}^n A_{PCM,i,j} \right)}_{\text{moisture transfer by convection from inner fabric to macroclimate air}} \quad (11)$$

Energy balance of macroclimate air:

$$\underbrace{\rho_{air} * e_{air} * A_{air} * \left(C_{air} * \frac{dT_{air,i}}{dt} - h_{fg} * \frac{dw_{air,i}}{dt} \right)}_{\text{transient storage term}} = \underbrace{\frac{T_{PCM,i,j} - T_{air,i}}{\frac{1}{h_c}} \sum_{j=1}^n A_{PCM,i,j}}_{\text{convective heat transfer from CM to macroclimate air}} + \underbrace{\sum_{j=1}^n \dot{m}_{ai,j} C_{air} (T_{ai,j} - T_{air,i})}_{\text{heat transfer by microclimate air ventilation}} + \underbrace{\left(\frac{T_{if,i} - T_{air,i}}{\left(\frac{R_{d,if}}{2} + \frac{1}{2 * h_c} \right) * \frac{r_{if}}{r_{if}}} \right) * \left(A_{if,i} - \sum_{j=1}^n A_{PCM,i,j} \right)}_{\text{convective heat transfer from inner fabric to macroclimate air}} + \underbrace{\left(\frac{T_{of,i} - T_{air,i}}{\left(\frac{R_{d,of}}{2} + \frac{1}{2 * h_c} \right)} \right) * A_{of,i}}_{\text{convective heat transfer from macroclimate air to outer fabric}} - \underbrace{\Psi * \lambda_{air,i} * h_{fg} * A_{air}}_{\text{heat released by condensation of water vapor}} \quad (12)$$

2.3. Integration of bio-heat and fabric-PCM model

The integration between the models was needed since the cooling vest performance is affected by the local torso skin temperatures. For each PCM-covered torso segment, the microclimate air average vapor pressures and temperatures were obtained from the PCM-fabric model as shown in Fig. 1 (b). Then, their values were used to predict the skin vapor pressure and temperature of the torso segment, while maintaining continuity of fluxes and skin temperatures at any time [5]. The procedure was followed for all the torso segments to find their corresponding skin temperatures. A mass balance was also performed to find the segmental vapor pressure of the skin, $P_{skin,i}$ [29], as follows:

$$P_{skin,i} = \left(\frac{P_{skin,i,sat}}{R_{e,skin}} + \frac{P_{a,j,avg}}{R_{e,a}} + \dot{m}_{sw,i} * h_{fg} \right) / \left(\frac{1}{R_{e,skin}} + \frac{1}{R_{e,a}} \right) \quad (13)$$

where $P_{a,j,avg}$, $P_{skin,i,sat}$, $\dot{m}_{sw,i}$, $R_{e,a}$ and $R_{e,skin}$ represent the average microclimate air vapor pressure, the segmental skin saturation pressure, the segmental sweat rate per unit area, the microclimate air evaporative resistance, and the skin evaporative resistance. If $P_{skin,i}$ was greater than $P_{skin,i,sat}$ then $P_{skin,i}$ was set to be equal to $P_{skin,i,sat}$.

2.4. Numerical solution

Fig. 2 presents a flowchart of the numerical methodology summarizing the simulation steps of the integrated fabric-PCM and bio-heat model to find the necessary number of packets and their arrangement on the torso.

The model takes as input the initial conditions and properties related the fabric-PCM and bio-heat models (working conditions, activity level, clothing type and PCM packets). The initial state of the human for the different unsteady simulations was found through the execution of the model for a long time to reach steady state in a preconditioned room

at 25 °C and 50% relative humidity [5,6,18]. After that, the number of packets needed for the inputted conditions was found by starting with a maximum of 20 packets and decreasing that number each time by 2 until the PCM melted fraction was above 85%. Once the number of PCM packets was found, the comfort level was determined when varying the placement of the packets on the torso segments; UF, LF and back. Using the explicit scheme with a time step equivalent to 0.02 s, the equations were solved over the desired simulation period (working duration) while looping over all the body segments.

The fabric-PCM model was only integrated to the segments covered with packets to find the micro and macro climate air temperatures and humidity content, fabric layers temperatures and regains and PCM temperatures and melted fractions. The detailed numerical solution of the fabric-PCM model can be found in the study of Itani et al. [6]. Then, the integrated model, through the average microclimate air temperature and vapor pressure found by the fabric-PCM model, predicted at each time step the skin temperatures, sweat rate and heat losses. Finally, Zhang et al.'s model [7] was utilized to find thermal comfort and sensation and the PCM arrangement that gives optimal comfort with a PCM melted fraction above 0.85 for effective use of the PCMs.

3. PCM arrangements and experimental methodology

The integrated model was validated with experimental data of human subjects performing activity at 3 MET in moderate environmental conditions of 35 °C ± 0.5 °C for an exercise period of 45 min. The subjects were wearing cooling vests with different placements of 14 PCM packets of 28 °C melting temperature or they were not wearing a vest. The number of PCM packets needed so that total melting of the packets did not occur was found using the methodology described in Section 2.4. According to the preliminary simulations, 12 PCM packets would be needed to ensure almost complete melting in 45 min. However, 14 packets were selected by design for the tests to make sure that total melting does not happen during experiments and hence accounting for any possible deviation in the model from real situation.

In the following subsections, an explanation is presented for the selected PCM arrangements for testing on the torso segments; UF, LF and back and for model validation, followed by the experimental procedure and recorded measurements.

3.1. PCM arrangements in the cooling vest

The cooling vest (SWEDE cooling vest) used in the current study is a commercially available medium size vest [25]. It was made of polyester with 20 pockets on its inner layer to hold up to 20 packets of the same dimensions with maximum of 10 packets on the front and 10 packets on the back [4,14]. The vest was also equipped with Velcro fasteners to adjust the size so as to fit the body of the participant.

Each PCM packet had a melting temperature, area, thickness, mass, density and heat of fusion of 28 °C, 80.24 cm², 8.75 mm, 87.5 g, 1239 kg/m³, and 159 kJ/kg, respectively [5]. The packets were kept at 20 °C to solidify overnight in an open wooden box in a climatic room.

As mentioned earlier, a total number of 14 PCM packets were used in the vest for the experiments and validation of the integrated model.

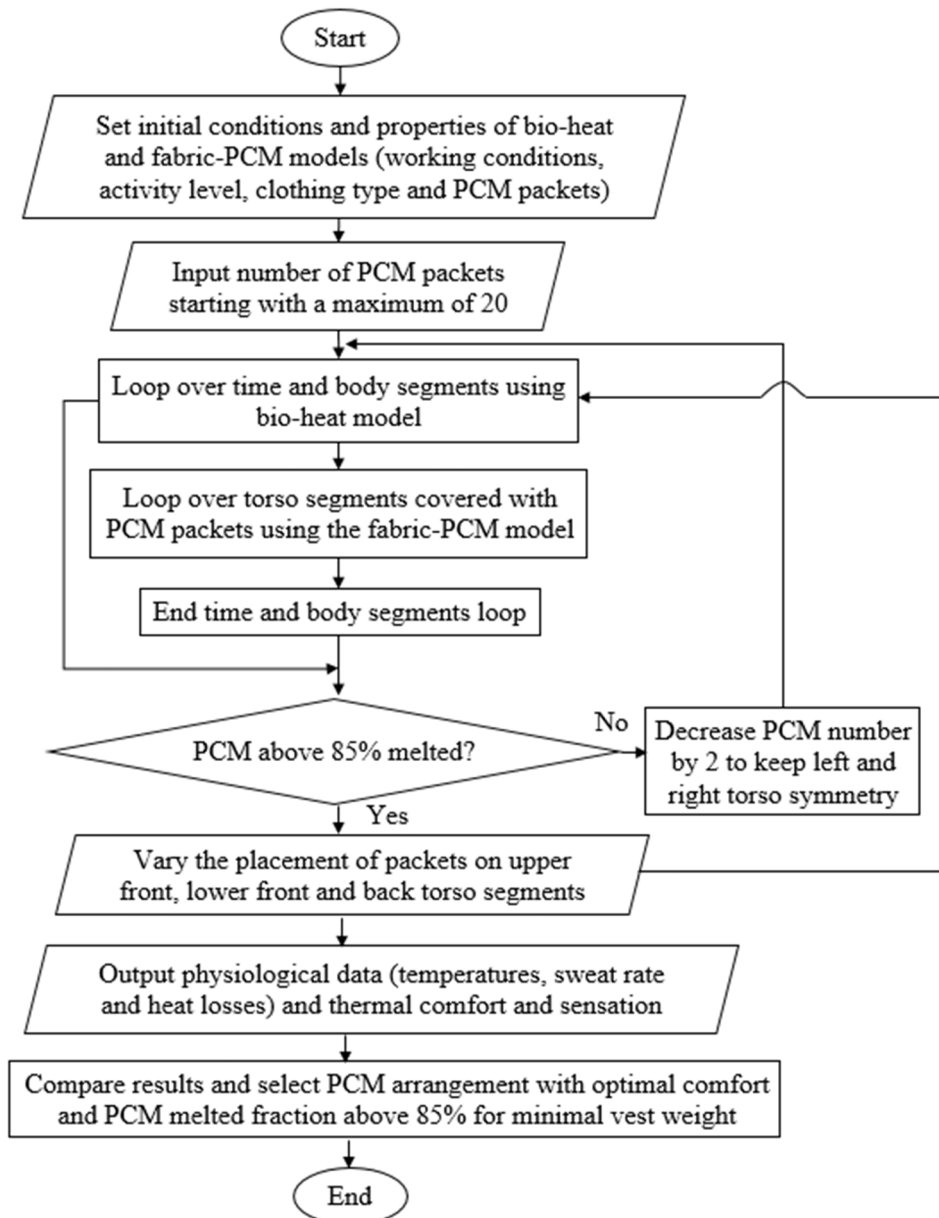


Fig. 2. Flowchart for the integrated model.

Given that the maximum number of packets that can be held on the back or the front was 10, the choice of 14 packets still allowed a significant variation in coverage area by the PCM between the UF, LF and back torso segments. Thus, the options of full 100% back/front coverage with partial front/back coverage were possible, in order to identify the optimal PCM placement on comfort. Back only cooling was reported to improve overall comfort compared to front only cooling at environmental temperature of 28 °C [17,19].

Seven different variations of the 14 PCM arrangements in the cooling vest were tested as presented in Table 1 and are shown in the schematics of Fig. 3 (a-f). These arrangements were tested experimentally on participants wearing the vest. The commercially available vest can hold a maximum of 10 PCM packets on the back, 6 on the UF and 4 on the LF torso segment. Thus, the PCM arrangement with 4UF-0LF-10B represented the case where 4 packets were positioned on the UF segment, 0 on the LF and the remaining 10 packets were positioned on the back, as shown in Fig. 3(a). In arrangement 2UF-2LF-10B, the number of packets on UF was decremented by 2 packets so that 2 packets were placed on UF, 2 on LF and the remaining 10 on the back,

as shown in Fig. 3(b). Thus, the effect of placing more packets on the UF or LF torso segments on comfort can be assessed. In arrangement 4UF-2LF-8B, the number of packets on UF was incremented by 2 while that at the back was decremented by 2, and so on for the remaining arrangements. Each PCM arrangement experimental test was repeated six times, along with the no PCM vest case. It should be noted that the effect of the carried vest weight on the subject metabolism who performed the experiments was minimal, as the weight of the PCM packets did not exceed 1.3 kg, resulting in estimated 3% increase in metabolic rate.

3.2. Participants

The approvals of the Institutional Review Boards at American University of Beirut and Qatar University allowed 6 healthy males to take part in the study. The sample size used in this study was found adequate based on the estimation using literature data for measured means and standard deviations in skin temperatures for paired groups [4,30]. In addition, the sample size is satisfactory for validating the

Table 1
PCM arrangements of the different experiments on the UF, LF and back torso segments.

PCM arrangement	PCM on UF	PCM on LF	PCM on back	Total PCM in vest
No vest	0	0	0	0
4UF-0LF-10B	4	0	10	14
2UF-2LF-10B	2	2	10	14
0UF-4LF-10B	0	4	10	14
4UF-2LF-8B	4	2	8	14
4UF-4LF-6B	4	4	6	14
6UF-4LF-4B	6	4	4	14

integrated model predictions as was done with one human subject for validating a similar bio-heat model in the study of Pokorný et al. [31]. Participants were provided with similar clothing having measured characteristics provided in Table 2 [32–35]. The intrinsic clothing thermal insulation shown in Table 2, is defined as the difference between the total insulation value for the clothing and the air layer

thermal resistance around the clothed thermal manikin [32]. The specific heat of the cotton and polyester fabric were taken from previous experimental collected data [36,37]. Moreover, the subjects had their own socks and shoes with properties estimated from standard data bases [38–40]. The participants with the help of a physician filled a questionnaire for physical activity and went through an ECG test to make sure they are healthy before selection. They were asked not to drink either alcohol or coffee for at least 24 h and not to eat or smoke for at least 2 h prior to the experiment. The average age of the participants was 21.5 ± 1.05 years (mean \pm SD), height was 1.75 ± 0.05 m and weight was 75.5 ± 7.7 kg.

During all the experiments, a nurse was present to watch the participants and intervene in case of any adverse event. The participants were briefed about the experiment and they signed a consent form before the experiments. Each participant contributed in seven experiments, one without a vest and six with a cooling vest of different PCM arrangements worn over the t-shirt, and on separate days with at least one day in between the experiments at a randomized order. The experiments were all performed in the afternoon of the months of

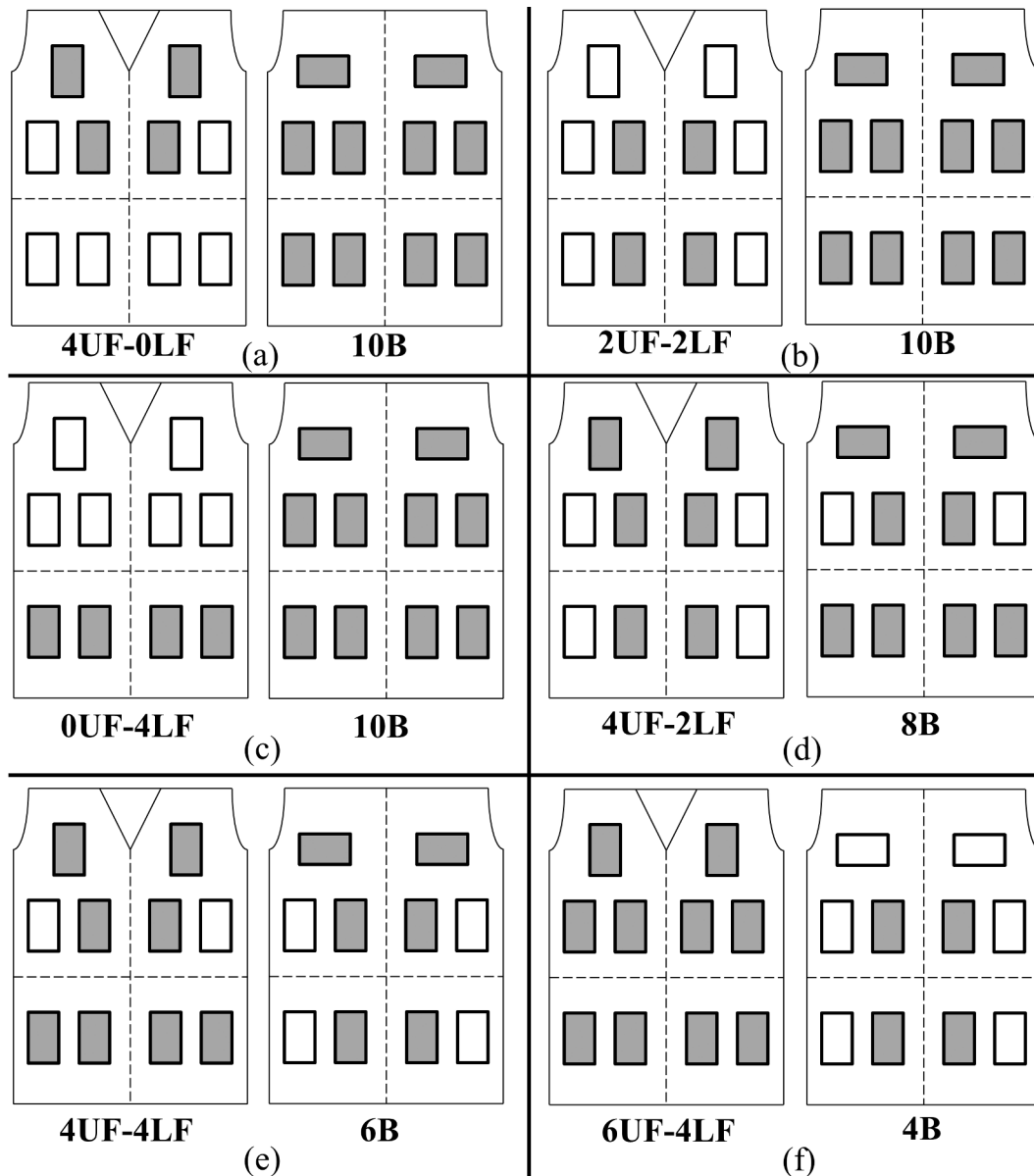


Fig. 3. Schematic showing the different PCM placement cases (a) 4UF-0LF-10B, (b) 2UF-2LF-10B, (c) 0UF-4LF-10B, (d) 4UF-2LF-8B, (e) 4UF-4LF-6B and (f) 6UF-4LF-4B.

Table 2
Clothing characteristics.

Clothing	Fiber content	Thickness (mm)	Area Density (g/m ²)	Intrinsic thermal insulation (m ² ·°C/W)	Evaporative resistance (m ² ·Pa/W)
Cooling vest	100% polyester	1.01 ± 0.01	824 ± 4	0.122 ± 0.030	35.0 ± 0.05
T-shirt	50% cotton & 50% polyester	0.56 ± 0.01	187 ± 1	0.042 ± 0.010	2.48 ± 0.02
Shorts	light cotton	0.91 ± 0.05	221.1 ± 10	0.014 ± 0.008	4.0 ± 0.3
Socks*	ankle-length, mainly cotton	2.87	386.7	0.004	13.6
Shoes*	thin-soled with some woven fabric and knit	3.50	900	0.004	52

* Average data from Fu [38], McCullough [39] and McCullough[40].

November and December with average ambient temperature of 20 °C and relative humidity of 60%.

3.3. Experimental procedure

The experimental climatic chamber was set at 35 °C ± 0.5 °C temperature and 50% relative humidity, representing a moderate environment [41]. The recorded air velocity in the chamber was 0.4 m/s, found using 731 A anemometer (accuracy of 3%).

Fig. 4 presents brief explanation of the experimental protocol followed by each participant in the experiments. After signing the consent form, the clothed participant was prepared and weighed. The PCM cooling vest, clothing, towel and equipment were also weighed separately. After preparing for the experiment in the lab, the participant rested for 30 min while seated to reach a steady physiological or thermo-neutral state [13,42]. At the end of the resting period, the participant put on the vest and entered the climatic chamber. Then, the participant cycled on a magnetic upright bike at 3 MET for 45 min while wearing the PCM vest. During the experiment, refreshments in the form of drinking water were provided for the participants in 0.5 L water bottles, however, no participant requested any.

A nurse took readings of the core temperature to ensure terminating the experiments if it surpassed 38 °C and avoid any ear damage, at the start and every 15 min throughout the exercise. Recording of subjective ratings was done on a designated sheet at the start and every 5 min during the experiments. After that, the participant exited the climatic chamber and was weighed together with their wet clothing and towel after drying off and then rested for a 10 min recovery period. The cooling vest, wet clothing and towel were also weighed separately after

the exercise ended.

To ensure that the participant was not subject to risk [43], the experiment was to be stopped when any of the following was applicable: (1) the core temperature became 38 °C (maximum temperature permissible under wet bulb globe temperature (WBGT) index according to ISO 9886 [44] and ISO 12894 [45]); (2) heart rate became 95% of the age predicted maximum heart rate (220-Age); or (3) subject wanted to end the experiments at any time. However, none of the participants in the current study requested to stop or was stopped by the researchers.

The above experimental procedure was also repeated by all the participants for the case when not wearing a cooling vest which represented the baseline for the comparison of vest performance.

3.4. Physiological and physical measurements

The weight of each subject, clothing, towel and different equipment was taken by the means of a bench scale (Quartzell™ Bench Scale 3600SC, Avery Weigh-Tronix – USA, 1 g resolution). The local skin temperature sensors (iButton® DS1922L, Maxim Integrated, CA, USA, resolution 0.0625 °C) were placed on seven segments on the left body side; on the upper arm, chest, abdomen, upper back, lower back, calf and thigh and were recorded every 5 min throughout the experiment. The average accuracy of the temperature sensors was ± 0.09 °C when used at the ambient conditions of 34.9 ± 0.1 °C with a maximum deviation of 0.4 °C [46]. A surgical tape was used to fix the sensors and ensure proper contact with the skin as previously done with these types of sensors [46,47]. The participant wore a wristband pulse oximeter (CMS-50F, accuracy ± 2%) to record their heart rate every 5 min throughout the experiment.

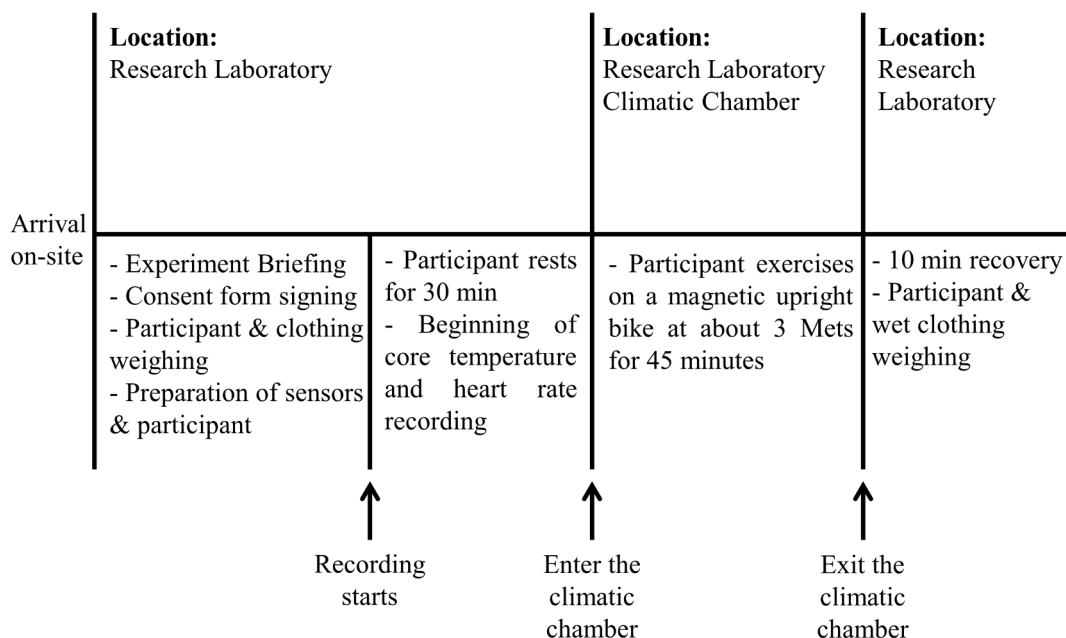


Fig. 4. Experimental procedure.

An infrared tympanic thermometer, IRTT, with disposable shields (Braun ThermoScan® 7 IRT6520, Braun, Kronberg, Germany, accuracy $\pm 0.2^\circ\text{C}$) was used to accurately measure core temperature of the participant, T_{cr} , and find the change in the core temperature from its initial state, ΔT_{cr} [48,49]. New generations of IRTTs were found to have good reliability in a recent study, when disposable shields were used and regular cleaning was done [50]. Furthermore, IRTTs are more time efficient, easily used, hygienic and acceptable to subjects or patients than rectal [50,51]. In this work, the same IRTT was utilized in all the experiments as a sign for ending the experiment with the assumption that any possible measurement error was equivalent in all experiments.

The change in mean skin temperature from its initial value, $\Delta T_{sk,mean}$, was calculated with $T_{sk,mean} = 0.3T_{chest} + 0.3T_{arm} + 0.2T_{thigh} + 0.2T_{leg}$ [52]. The front and back skin temperatures were calculated by finding the average of the chest and abdomen and upper and lower back, respectively [14,53,54]. The front and back skin temperatures were recorded through measurements on four torso locations to ensure good representation of the torso regions that are either covered by the packets or not. In addition, the sensors were placed on the left side of the torso only assuming a symmetry between the left and right sides of the torso segments. Body weight loss or sweat production was found from the weight change of a clothed participant before and after the exercise and corrected for sweat absorbed in the clothing and towel [55].

3.5. Subjective ratings and statistical analysis

Recording of subjective ratings was done every 5 min for overall thermal comfort, TC and torso thermal sensation, TTS . The reference scales for the subjective ratings are shown in Table 3 and were used previously in many studies [14,56–58]. In order to compare Zhang's model predictions on a 5-point scale of thermal comfort (very uncomfortable at -4 to neutral at 0) and sensation (neutral at 0 to very hot at +4) to the experimental ones on a 6-point scale, a proportional relationship was assumed between the two scales, with a ratio of proportionality of 1.25.

Paired-samples t tests were used to assess and analyze the effect of wearing a vest on the measured parameters in the study. A value of $p < 0.05$ was set for statistical significance [4,59]. In addition, if significant effect was found, Cohen's d post-hoc test was utilized to find the effect size and get an idea about the magnitude of the cooling vest effect [60].

4. Results and discussion

In the coming subsections, the experimental human subject results will be analyzed and compared to those predicted by the integrated model for its validation. This will be followed by case studied to determine the extent of thermal comfort improvement associated with optimal PCM arrangements at fixed number of PCM packets and melting temperature for different durations and ambient conditions.

4.1. Validation of integrated model via human subject testing

4.1.1. Heart rate

The heart rate increased from an initial value at rest of about 68 ± 8 bpm to reach 126 ± 6 bpm at the end of the experiment in the no vest case, 87 ± 4 bpm in arrangement **2UF-2LF-10B** and 92 ± 4 bpm in arrangement **4UF-0LF-10B**. Only arrangements **4UF-0LF-10B** and **2UF-2LF-10B** were significantly different ($p < 0.05$) from the no vest one.

4.1.2. Local and mean skin and core temperatures

The experimental and simulation results for the transient variation of the front and back torso skin temperatures are provided in Fig. 5(a) and (b), respectively, for the different experiments. In addition, Fig. 5(c) shows experimental and simulation results of the back skin

temperature at the end of the experiment, in order to visualize the effect of PCM coverage on the back skin temperature. The local skin temperatures of the no vest case had an increasing trend reaching their highest values at the end of the experiment and was also predicted by the integrated model. On the other hand, the cooling vest cases showed a drop in the local torso skin temperatures in the first 10 min followed by an increase in the skin temperatures to reach their final states. Thus, the model predicted the transient variation of the skin temperatures when either covered with PCM packets or not. In the no vest case, the front torso skin temperature reached a maximum value of $36.13^\circ\text{C} \pm 0.24^\circ\text{C}$, while that of the back torso segment reached $34.89^\circ\text{C} \pm 0.43^\circ\text{C}$.

Upon varying the arrangement of the PCM packets on the UF, LF and back, a difference was detected between the segmental skin temperatures as the PCM coverage area increases. For example, as the PCM coverage area increased on the back segment from 40% in arrangement **6UF-4LF-4B** to 100% in arrangement **2UF-2LF-10B**, the back skin temperature showed a linear drop and had a difference of $3.21^\circ\text{C} \pm 0.49^\circ\text{C}$, as shown in Fig. 5(c), while the front showed a drop of $1.47^\circ\text{C} \pm 0.44^\circ\text{C}$. This difference in skin temperatures, as the coverage area increased, was captured by the integrated model to an acceptable degree of accuracy with maximum deviation throughout the exercise period of $\pm 0.78^\circ\text{C}$ and $\pm 0.66^\circ\text{C}$ in front and back skin temperatures, respectively. Moreover, the highest drop in back temperature from the no vest case was with arrangement **4UF-0LF-10B** that showed a $3.87^\circ\text{C} \pm 0.6^\circ\text{C}$ temperature drop, while the model predicted accurately a drop of 3.6°C .

The arrangements with fixed PCM coverage on the back while varying the coverage on UF and LF segments (**0UF-4LF-10B**, **2UF-2LF-10B** and **4UF-0LF-10B**) showed similar back skin temperatures, however, lower front skin temperatures were attained as the coverage area on the UF segment increased (Fig. 5(a)). During the full exercise period, the front skin temperature corresponding to arrangements **4UF-2LF-8B**, **4UF-4LF-6B** and **6UF-4LF-4B** were significantly lower ($p < 0.05$) than the no vest arrangement except for the front skin temperature corresponding to arrangements **0UF-4LF-10B**, **2UF-2LF-10B** and **4UF-0LF-10B**. As for the back skin temperature, arrangements **0UF-4LF-10B**, **2UF-2LF-10B** and **4UF-0LF-10B** were the only configurations significantly different from the no vest case throughout the exercise period. The effect size estimated using Cohen's d [60] was found to have a value of about 1.6, which indicates a large magnitude of the cooling vest effect. The two arrangements **4UF-0LF-10B** and **6UF-4LF-4B** were the ones that resulted in the lowest back and front skin temperatures, respectively, after 45 min of exercise. It was noted that total melting of the packets did not occur with 14 PCM packets at moderate conditions of 35°C and for a 45 min exercise period.

The experimental change in mean skin temperature, $\Delta T_{sk,mean}$, in all the cases had an increasing trend with time. The maximum $\Delta T_{sk,mean}$ corresponded to the no vest arrangement $3.48 \pm 0.5^\circ\text{C}$ at the end of the experiment. In all the cooling vest cases, a drop in $\Delta T_{sk,mean}$ from the no vest case was found, with a statistically significant difference from the no vest arrangement ($p < 0.05$) in the last 15 min of exercise in all the cases. With respect to the change in the core temperature, similar trend of variation to the mean skin temperature was found, however, no significant difference existed in ΔT_{cr} at all times throughout the exercise

Table 3
Reference scales for subjective ratings.

No. scale	TC scale	TTS scale
0	comfortable	Neutral
1	just comfortable	slightly warm
2	slightly uncomfortable	Warm
3	uncomfortable	Hot
4	very uncomfortable	very hot
5	extremely uncomfortable	extremely hot

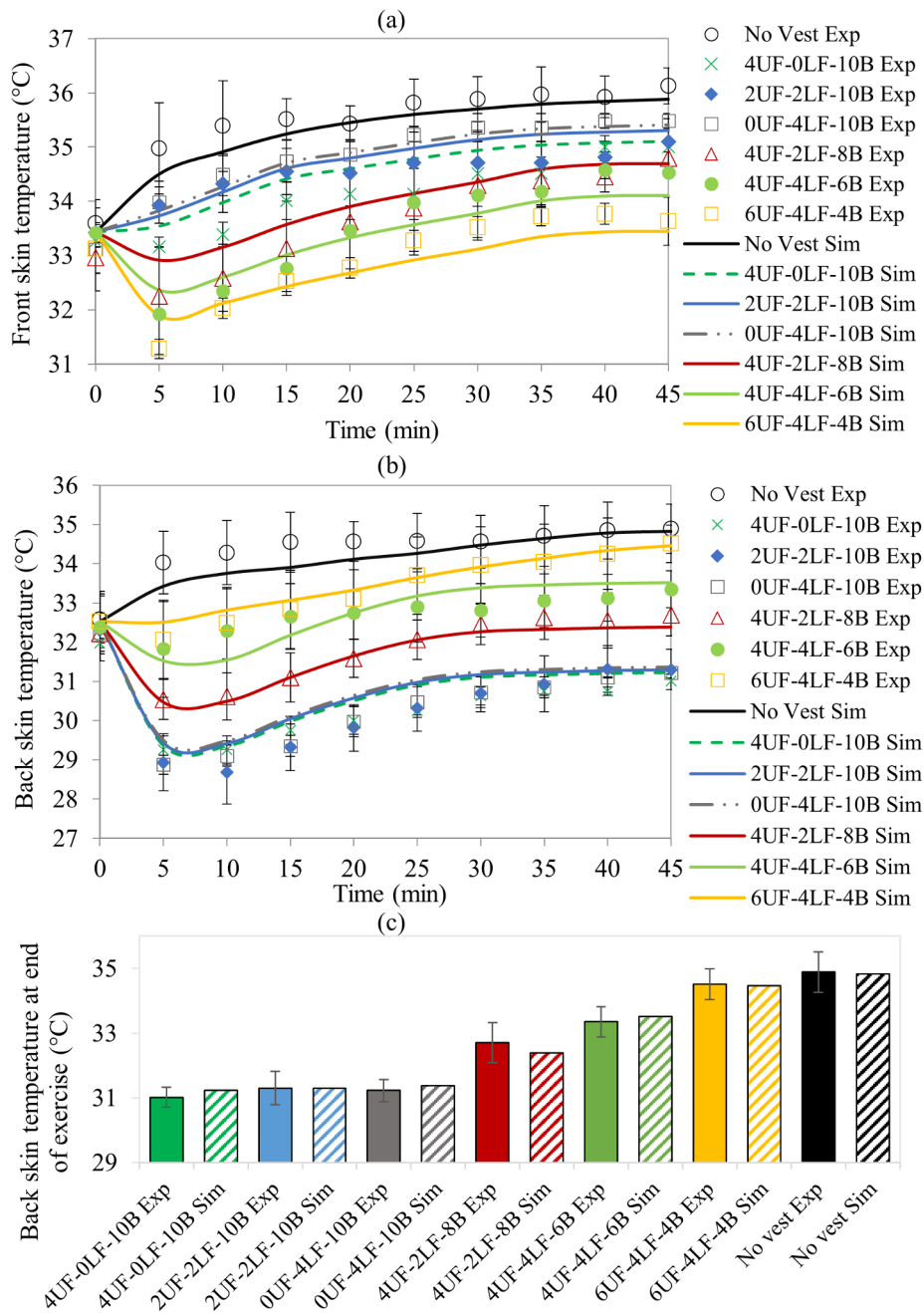


Fig. 5. Experimental (mean values \pm SD) and simulation results of (a) front local skin temperature, (b) back local skin temperature during 45 min exercise and (c) back skin temperature at the end of experiment for the different cases.

between the different cases. The above results signified that a detectable difference was found between the different PCM arrangements, but mainly in local torso skin temperatures.

4.1.3. Body weight loss

The body weight loss or sweat production measured (solid fill bar) at the end of the 45 min exercise of the different experiments (Table 1) and for the predicted values by the model simulation (hatched bar) are shown in Fig. 6. The simulation results of the integrated model showed good agreement with the experimental ones, with about a 14% maximum error from the mean experimental values, shown in Fig. 6. In the presence of a cooling vest, the amount of sweat decreased as compared to the no vest that was at 0.35 ± 0.05 kg. Only sweat produced in arrangements 4UF-0LF-10B, 2UF-2LF-10B, 0UF-4LF-10B and 4UF-2LF-8B was significantly different from the no vest case ($p < 0.05$).

Therefore, the back segment, as was previously found in literature, is a body region that suppresses sweat production when cooled [6,8]. The results were also in agreement with the conclusions reported Choi et al. [61], where a reduction was observed in total sweat rate when wearing a cooling vest while harvesting red pepper for two hours and the drop in torso and mean skin temperatures improved thermal sensation. Furthermore, Webster et al. [76] reported enhanced thermal state and some reduction in core temperature rise in athletes running for 30 min at 37 °C due to 35 min pre-cooling using an ice cooling vest.

4.1.4. Thermal comfort and sensation

The mean experimental subjective ratings and simulation results of TTS and TC are shown in Fig. 7(a) and (b), respectively. In addition, Fig. 7(c) shows experimental and simulation results of TC at the end of exercise period, in order to visualize the effect of PCM coverage as it

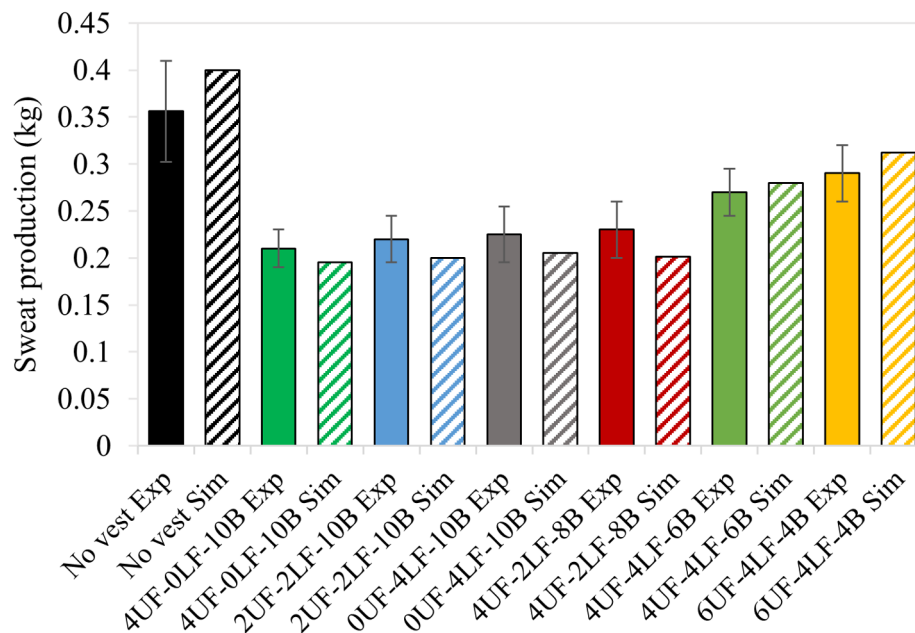


Fig. 6. Mean experimental values and SD (solid fill bars) and predicted values by simulation (hatched bars) of sweat production after exercise.

was varied on the torso segments. The ratings of *TTS* and *TC* kept on increasing in all the cases reaching the highest values of 4.3 ± 0.53 (between very and extremely hot) and 4.5 ± 0.5 (very uncomfortable), respectively, in the no vest case. When wearing the vest, the rate of increase of *TTS* and *TC* with time was lower than that of the no vest, which was also predicted by the simulation model. Variation of the PCM coverage area on the torso segments have led to a detectable difference in local skin temperatures and this was reflected in the *TTS* and *TC* experimental and model results. As the PCM coverage area increased from 40% to 100% on the back segment, while decreasing on the front, *TTS* linearly improved from 4 ± 0 (very hot) to 2 ± 0.5 (warm) (Fig. 7(a)) and *TC* almost linearly improved from 3.67 ± 0.6 (uncomfortable) to 1.75 ± 0.5 (slightly uncomfortable), as presented in Fig. 7(b) and (c). This difference in ratings was captured by the model predictions, where *TTS* and *TC* improved from 3.71 (hot) to 2.42 (warm) and from 3.5 (uncomfortable) to 2.15 (slightly uncomfortable) with maximum deviations from mean experimental data of ± 0.7 and ± 0.8 , respectively. During all the exercise period, *TTS* and *TC* corresponding to arrangements 4UF-0LF-10B, 2UF-2LF-10B, 0UF-4LF-10B, were significantly lower than the no vest case ($p < 0.05$).

However, it was noticed among those cases that as the PCM coverage area was increased on the UF segments while decreasing it on the LF and fixing it on the back, *TC* and *TTS* were improved. *TC* corresponding to arrangements 4UF-2LF-8B, 4UF-4LF-6B and 6UF-4LF-4B was significantly different ($p < 0.05$) in the last 15 min of exercise from the no vest case but there was no significant difference in *TTS*. Thus, as the PCM coverage area increased on the back, improvements in overall comfort and torso sensation were significant. In addition, placing more packets on the UF segment showed improved *TC* over more coverage on the LF segment, while having full coverage on the back.

The above results were predicted with good accuracy by the integrated model, having a maximum difference from experimental data of ± 0.78 °C, 14% and ± 0.8 in local skin temperatures, sweat rate and thermal comfort and sensation, respectively. The accuracy of the model was similar to that of previous studies utilizing similar bio-heat models [33]. The extent of comfort improvement can be evaluated by the difference between the two arrangements with highest and lowest PCM coverage area on the back and vice versa on the UF and LF segments. These two arrangements had no significant difference in sweat rate, mean skin and core temperatures, however, the model detected a

difference by 1.66 °C and 3.23 °C in local back and front skin temperatures, respectively. This difference in skin temperatures was reflected in *TTS* and *TC* results with a magnitude of improvement by 1.29 and 1.35, respectively, as the coverage area increased on the back while the remaining packets covered the UF segment. From the findings of this study, it can be concluded that after the back and in order to have highest improvement in comfort, the UF torso segment should be first covered with PCM packets followed by the LF one. In addition, the results prove the robustness of the model for use in determining improvements in thermal and comfort states of an active human wearing cooling vest in presence of PCM asymmetry between UF, LF and back segments.

4.2. Application of the modeling approach to optimize PCM placement at other working durations and environmental conditions

4.2.1. Description of considered case studies

The integrated model was shown to be capable of detecting the difference in human thermal responses and subjective ratings under different arrangements of packets on the torso segments; UF, LF and back. However, application of the proposed modeling approach was needed to investigate similar differences at other working durations and environmental conditions for selected PCM melting temperature. Using the model, the minimum number of packets (minimum weight) and their placement in the vest to achieve overall comfort was found, as was described in Section 2.4. The packets were distributed on the torso segments; UF, LF and back, and should be almost totally melted at the end of exercise.

The case studies considered an active human at a metabolic rate of 3 MET in two environments; a moderate environment of 35 °C and 50% relative humidity and a hot environment of 40 °C and 40% relative humidity. It was assumed that the human started activity after resting at 0.8 MET for a long period to reach a steady physiological state in a preconditioned space at 25 °C and 50% relative humidity. Three working durations of 45, 60 and 90 min were considered at the moderate environment and two working duration of 45 and 60 min were considered at the hot environment. These durations are common for different moderate activity tasks (exercising, walking, gardening, etc.) and have been used in previous studies [42,62,63]. A longer working duration at the hotter environment was not selected since working

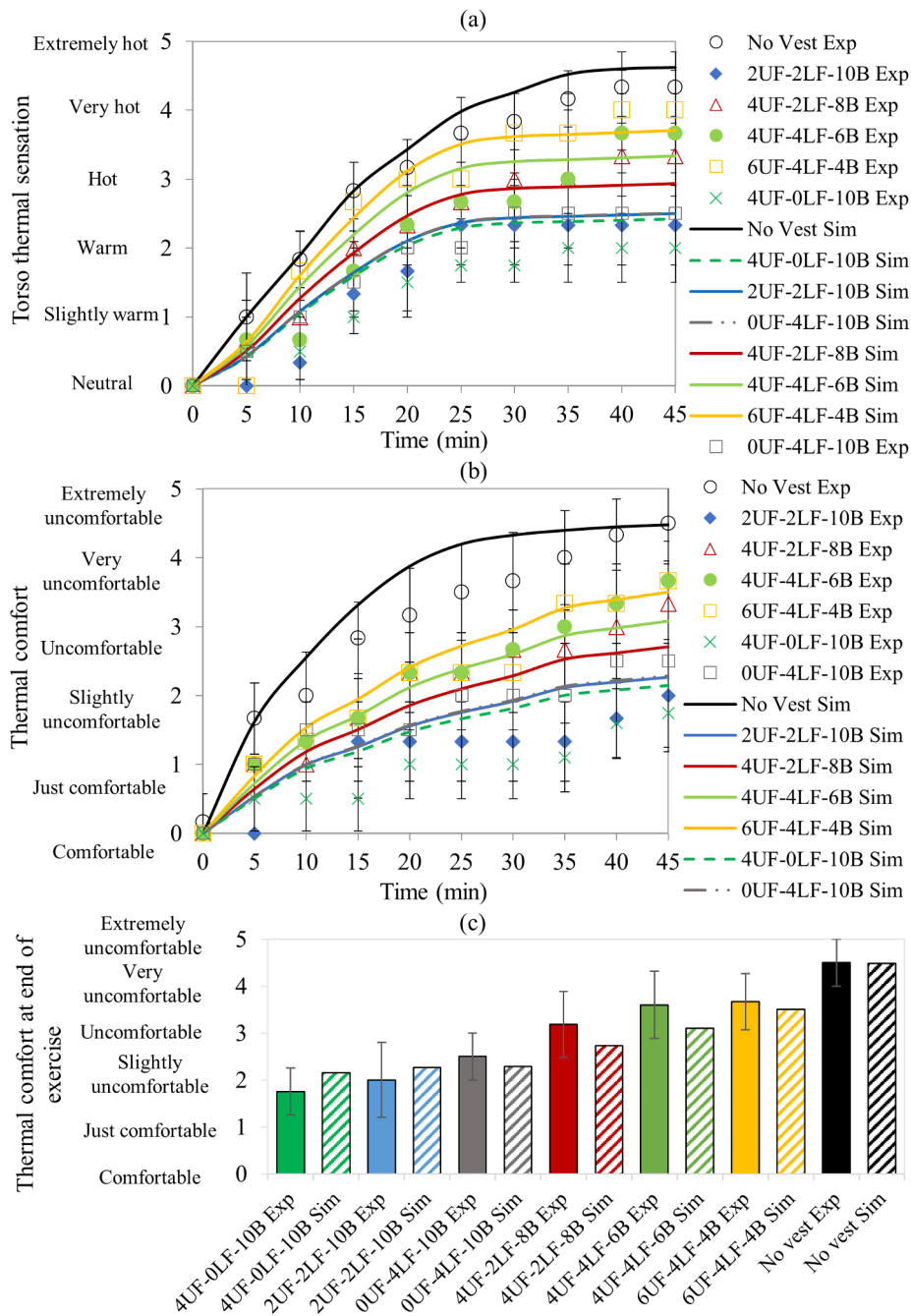


Fig. 7. Experimental (mean values \pm SD) and simulation results of (a) torso thermal sensation, (b) thermal comfort during exercise and (c) thermal comfort at end of exercise.

periods longer than one hour might be reported to cause heat stresses to the workers [64,65].

At the moderate environment, the human wearing a vest with PCM packets of 28 °C melting point was used, identical to the commercially available ones described in Section 3.1. The use of 28 °C packets at the moderate environment resulted in improvement in comfort and sensation without fully covering the torso [4,6] and hence PCM coverage area and arrangement on torso segments could be varied for different working durations. To have a significant cooling effect at hotter environments while allowing for variation in PCM arrangement in the cooling vest (coverage area is not 100%), a lower PCM melting temperature was recommended at 18 °C packets [13]. Hence, at the hotter environment, the selected PCM packets melting temperature, density and latent heat of fusion were 18 °C, 1169 kg/m³ and 113 kJ/kg,

respectively.

The number of PCM packets needed was first determined such that the melted fraction was above 85% using the methodology outline in Section 2.4. At the moderate environment of 35 °C, the obtained number of 28 °C PCM packets for the working duration of 45, 60 and 90 min were 12 (60% of torso covered), 14 (70% of torso covered) and 16 (80% of torso covered) with a predicted corresponding melted fraction of 0.95, 0.88 and 0.96, respectively. At the hot condition of 45 °C and working durations of 45 and 60 min, the required number of 18 °C PCM packets was 12 (60% of torso covered) and 16 (80% of torso covered), with a predicted melted fraction of 0.9 and 0.94, respectively. At both environments, increasing the working duration required additional PCM packets to achieve the required cooling effect and improvement in comfort.

After finding the necessary packets for each condition, the number of packets covering the torso segments; UF, LF and back, were varied. This variation allowed the finding of the PCM arrangement that would give the best thermal comfort and sensation, keeping in mind that a maximum of 10, 6 and 4 packets can cover the back, UF and LF, respectively. The minimum number of packets covering the front was 2 and then increased by increments of 2, while decreasing coverage on the back by 2 to maintain a constant total number of packets, as summarized in Table 4, for the 45 min working duration at both environments. The same procedure was followed for the remaining working durations (see Table 4). Thus, the resulting total number of simulations was 48 which represented the different PCM arrangements on the segments; UF, LF and back, in addition to the no vest case. The overall thermal comfort at the end of the work period were computed for all the different cases. Based on the highest (optimal) and lowest (worst) improvement in thermal comfort and torso sensation from the no vest case, the optimal and worst PCM arrangements were identified for each working duration and environmental condition.

4.2.2. Results of simulation cases

The variation of front and back skin temperatures for the no vest case and the optimal PCM arrangements for the different working durations are shown for the moderate environment in Fig. 8(a) and (b), respectively, and for the hot environment in Fig. 8(c) and (d), respectively. At the moderate environment and working durations of 45, 60 and 90 min, the 28 °C PCM coverage area on the torso was 60%, 70% and 80%, respectively. The optimal PCM arrangement upon varying the working duration and the coverage area was the one that considers full coverage of the back segment (10 PCM packets), and the remaining packets would only cover the UF segment. Consequently, the worst arrangements were those with full coverage on the UF and LF and

minimum on the back. However, placing 8 packets on the back showed slightly higher TC and TTS, which implied selecting the full coverage on the back as the optimal arrangement. The local skin temperatures in the no vest cases had an increasing trend with time, however, the rate of increase was reduced in the PCM vest cases. In the first 10 min, significant initial effects of the relatively low PCM temperature on skin temperatures were noticed in the cases where the PCM coverage area was substantial (6 packets and above) as shown in Fig. 8(b), and more significantly with the 18 °C packets, as shown in Fig. 8(d). After that, the skin temperatures increased to reach almost stable values during the PCM melting period. It can be noticed that at the hot environment, higher drops in skin temperatures occurred due to higher temperature differences between the skin and melting point of the PCM packets [5].

In an ascending order of improvement, the predicted TC at the end of the 60-min work period for the different PCM arrangements at moderate environment of 35 °C and hot environment of 40 °C are shown in Fig. 9(a) and (b), respectively. It was evident that for the different working durations and ambient conditions, the presence of the cooling vests achieved significant improvements in TC over the no vest case, which were almost extremely uncomfortable. At both environments, the results showed that more improvement in TC was attained as the coverage area on the back increased from 40% to 100% at the moderate environment and from 60% to 100% at the hot environment. Moreover, increasing the PCM packets on the UF segments while decreasing them on the LF segments and fixing the packets on the back (4UF-0LF-10B, 2UF-2LF-10B and 0UF-4LF-10B), showed more improvement in TC, as shown in Fig. 9(a) for the moderate environment and in Fig. 9(b) for the hot environment (6UF-0LF-10B, 4UF-2LF-10B and 2UF-4LF-10B). However, that improvement was more noticeable at the hot environment due to lower PCM melting temperature covering the torso segments. Therefore, the segment that was most influential on improving

Table 4
Simulation cases at different environmental conditions and working durations.

35 °C environment					40 °C environment				
Case	PCM on UF	PCM on LF	PCM on Back	Total PCM in Vest	Case	PCM on UF	PCM on LF	PCM on Back	Total PCM in Vest
<i>45-min working duration</i>									
No vest	0	0	0	0	No vest	0	0	0	0
2UF-0LF-10B	2	0	10	12	2UF-0LF-10B	2	0	10	12
0UF-2LF-10B	0	2	10	12	0UF-2LF-10B	0	2	10	12
4UF-0LF-8B	4	4	8	12	4UF-0LF-8B	4	4	8	12
2UF-2LF-8B	2	2	8	12	2UF-2LF-8B	2	2	8	12
0UF-4LF-8B	0	4	8	12	0UF-4LF-8B	0	4	8	12
6UF-0LF-6B	6	0	6	12	6UF-0LF-6B	6	0	6	12
4UF-2LF-6B	4	2	6	12	4UF-2LF-6B	4	2	6	12
2UF-4LF-6B	2	4	6	12	2UF-4LF-6B	2	4	6	12
6UF-2LF-4B	6	2	4	12	6UF-2LF-4B	6	2	4	12
4UF-4LF-4B	4	4	4	12	4UF-4LF-4B	4	4	4	12
6UF-4LF-2B	6	4	2	12	6UF-4LF-2B	6	4	2	12
<i>60-min working duration</i>									
No vest	0	0	0	0	No vest	0	0	0	0
4UF-0LF-10B	4	0	10	14	6UF-0LF-10B	6	0	10	16
2UF-2LF-10B	2	2	10	14	4UF-2LF-10B	4	2	10	16
0UF-4LF-10B	0	4	10	14	2UF-4LF-10B	2	4	10	16
6UF-0LF-8B	6	0	8	14	6UF-2LF-8B	6	2	8	16
4UF-2LF-8B	4	2	8	14	4UF-4LF-8B	4	4	8	16
2UF-4LF-8B	2	4	8	14	6UF-4LF-6B	6	4	6	16
6UF-2LF-6B	6	2	6	14					
4UF-4LF-6B	4	4	6	14					
6UF-4LF-4B	6	4	4	14					
<i>90-min working duration</i>									
No vest	0	0	0	0					
6UF-0LF-10B	6	0	10	16					
4UF-2LF-10B	4	2	10	16					
2UF-4LF-10B	2	4	10	16					
6UF-2LF-8B	6	2	8	16					
4UF-4LF-8B	4	4	8	16					
6UF-4LF-6B	6	4	6	16					

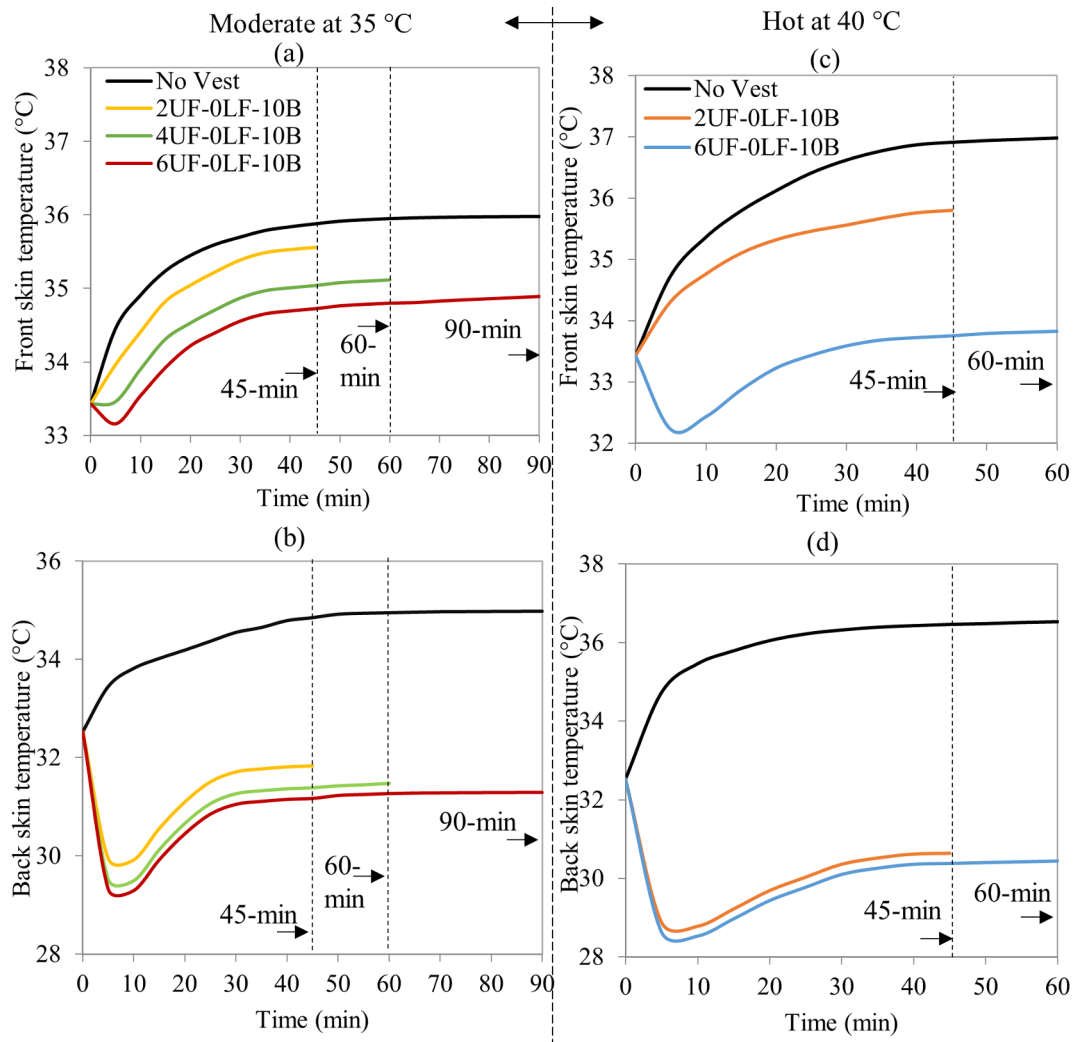


Fig. 8. Plots showing simulation results of (a) front and (b) back skin temperatures at moderate environment and (c) front and (d) back skin temperatures at hot environment, for the no vest case and optimal PCM arrangements for different working durations.

TC was the back, as was previously reported in literature [6,8]. Following the back, the UF and then the LF segment was found to be more influential on comfort improvement at both studied ambient conditions.

The predicted *TTS* and *TC* of the no vest at the end of the different working durations, worst and optimal PCM arrangements are shown in Fig. 10(a) and (b), respectively. For the different working durations and ambient conditions, the presence of the cooling vests achieved significant improvements in *TTS* and *TC* above the no vest condition. At the moderate environment, when 60% of the torso is covered with PCM, the worst arrangement reduced the improvement in *TTS* and *TC* by about 24% and 18%, respectively, and by 17% and 13% when the torso was 80% covered. However, at the hot environment, when 60% (or 80%) of the torso is covered with PCM packets, the worst arrangement reduced the improvement in *TTS* and *TC* by about 11% and 23% (or 6% and 16%), respectively. Therefore, the variation in PCM arrangement on torso segments (UF, LF and back) showed higher differences in *TTS* and *TC* between the worst and optimal arrangements with lower coverage areas, in both environments.

Table 5 summarizes the differences in local skin temperatures, *TTS* and *TC* for the optimal arrangements and for the worst arrangements for comfort at different working durations and conditions. In assessing the differences between the optimal and worst cases, the detected time-

averaged difference in front and back skin temperatures ($\Delta TF_{o,w,avg}$ and $\Delta TB_{o,w,avg}$) was 1.94 °C and 2.51 °C, respectively, for a 45-min working duration. These differences in front and back skin temperatures at the end of the working period ($\Delta TF_{o,w,end}$ and $\Delta TB_{o,w,end}$) were 1.82 °C and 2.78 °C, respectively. Regarding the detected time-averaged difference in *TTS* and *TC* ($\Delta TTS_{o,w,avg}$ and $\Delta TC_{o,w,avg}$) between optimal and worst cases, the results were 0.81 and 0.7, respectively, for a 45 min working duration. At the end of the 45 min, the difference in *TTS* and *TC* ($\Delta TTS_{o,w,end}$ and $\Delta TC_{o,w,end}$) between optimal and worst cases were 0.6 and 0.4, respectively. As the working duration increased from 45 to 90 min at the moderate environment, these difference were less prominent due to the higher PCM coverage area needed at longer durations. Thus, as the coverage area increased from 60% to 80%, the difference in local skin temperatures, *TTS* and *TC* between optimal and worst cases reduced. Moving to the hot environment, the 18 °C melting point PCM coverage area on the torso was 60% and 80% for the 45 and 60 min working durations, respectively. Similar to the moderate environment, the optimal arrangements upon varying the working duration at the hot environment were those considering full coverage of the back and the remaining packets on the UF segment. In addition, at the 45 min working duration, $\Delta TF_{o,w,end}$ and $\Delta TB_{o,w,end}$ were higher than those at the moderate environment, since a lower PCM melting

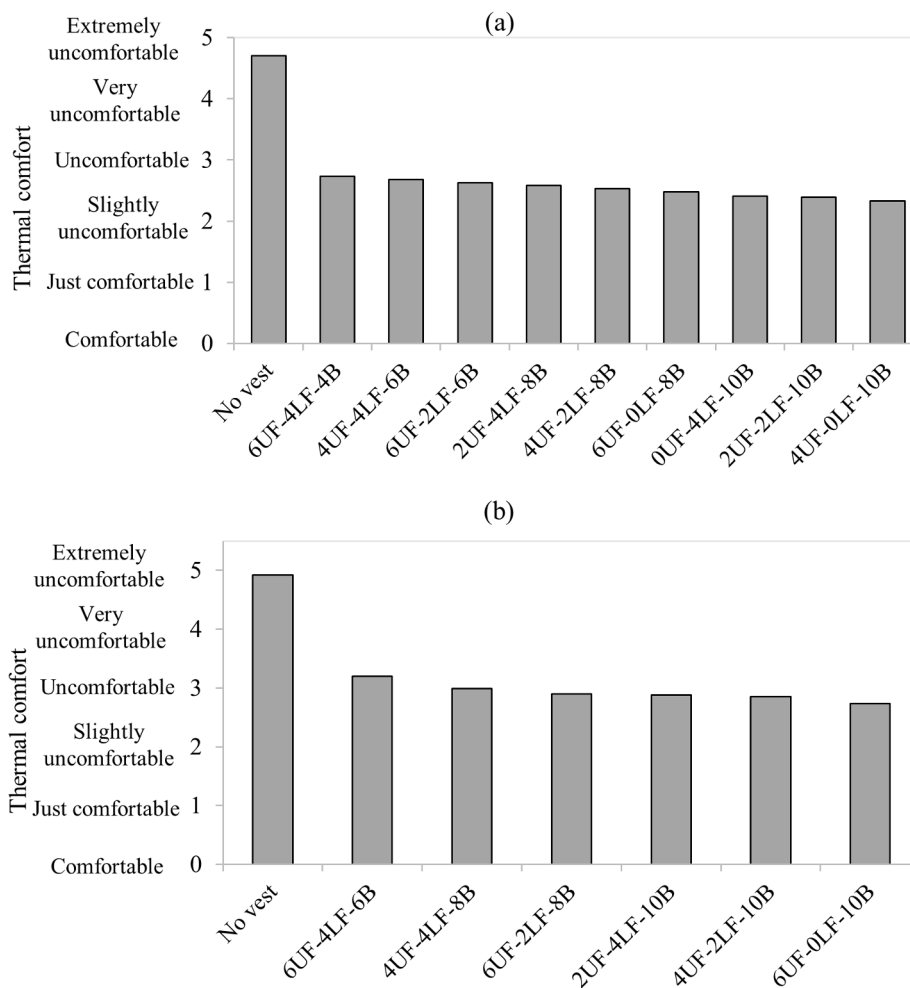


Fig. 9. Plots showing simulation results of TC for the 60 min working duration at (a) moderate environment of 35 °C and (b) hot environment of 40 °C in ascending order of improvement.

temperature was used. As the working duration and the PCM coverage area increased, the difference in local skin temperatures, TTS and TC between optimal and worst cases decreased.

The findings of the simulated cases agree with the experimental ones, which showed that with a limited number of PCM packets, placing more packets on the back segment, followed by the UF and then LF segments, is an effective approach when body cooling is needed, while asymmetry exists between front and back. The integrated model was capable of detecting the difference in comfort and sensation of an active human, upon varying the PCM arrangement on the UF, LF and back segments. It was also found that increasing the PCM packets on the UF segment while decreasing them on the LF segment and fixing the packets on the back showed larger improvements in TC . However, that improvement was more noticeable at the hotter environment due to lower PCM melting temperature covering the torso segments. In previous studies on the relative importance of different body regions for thermal comfort of humans [9,10], local cooling of the abdomen (LF) did not show significant improvement in thermal comfort, while local cooling of the upper and lower back segments did. This explains why, in the current study, the improvement in TC was more noticeable when the lower melting temperature packets were placed on the UF and not on the LF in the hot environment. Zhang et al. [7] found that when the body was warm, cooling the UF segment would provide higher comfort than cooling the LF segment. In addition, Itani et al. [19] reported that locating the PCM packets on the back led to a better thermal sensation.

5. Conclusion

This study assessed the importance of PCM arrangement in a cooling vest on improving comfort and thermal responses of active human at different working durations and climates. Experiments were done on six male subjects, which included cycling on a bike at 3 MET for 45 min at a moderate environment of 35 °C and 50% relative humidity. The experimental findings were used to validate an integrated bio-heat and fabric-PCM model which proved its capability in detecting a difference in thermal responses and comfort sensations upon varying the PCM arrangement of a fixed number of packets on the torso segments; UF, LF and back. Application of the modeling approach was done for specific PCM melting temperatures at different working duration and environmental conditions, to find the needed number of packets and the optimal arrangement on the torso segments.

The findings of the study showed that local cooling of the torso when full coverage is not needed and with a limited number of PCM packets, placing more packets on the back, followed by the UF and then LF, would show the optimal improvement in thermal comfort. Cooling the LF segment did not show significant improvement in comfort over cooling the UF segment, which was more evident when cooling with lower PCM packets at the hot environment. Smaller differences in skin temperatures and comfort between the optimal and worst cases were detected as the working duration increased, since higher PCM coverage area was needed. The findings of the study could be extended to

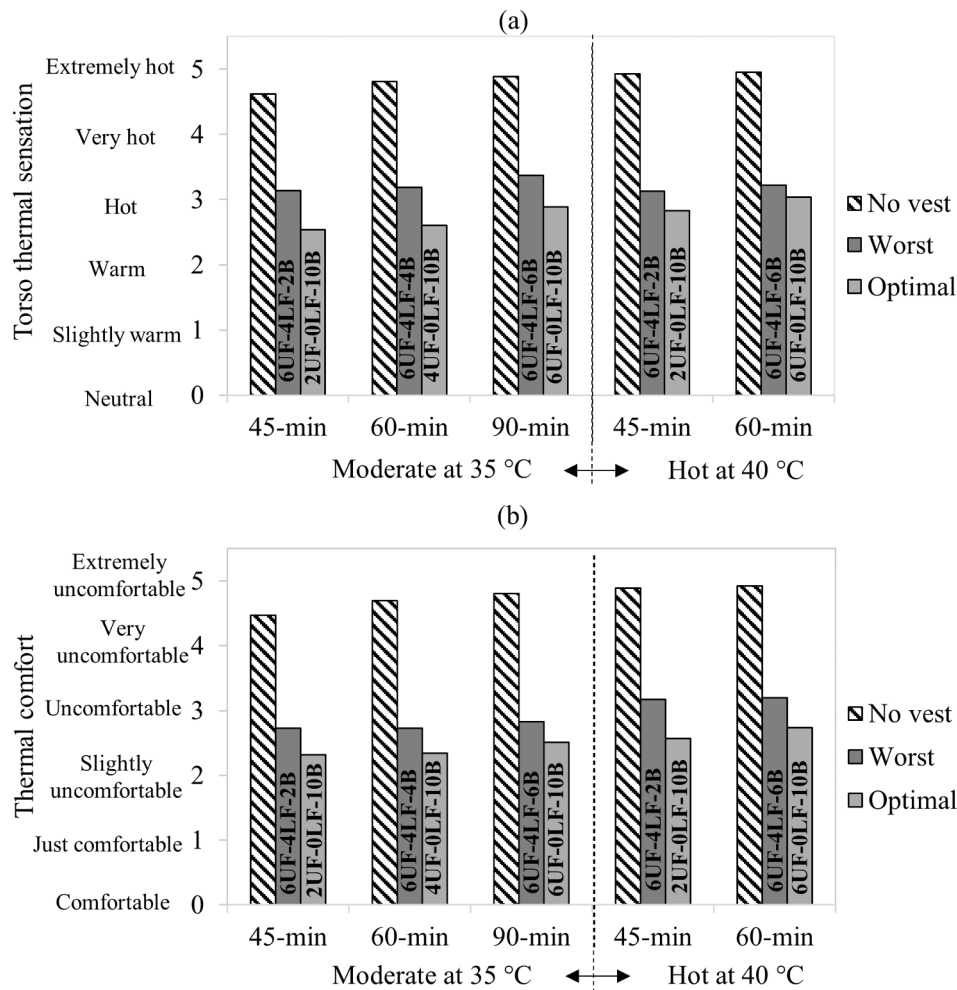


Fig. 10. Plots showing simulation results of (a) TTS and (b) TC for no vest, worst and optimal PCM arrangements at different working conditions.

Table 5

Optimal and worst cases at different working conditions with main differences in skin temperatures, comfort and sensation averaged over the entire working period and the values at the end.

Environment	Moderate at 35 °C			Hot at 40 °C	
	45 min	60 min	90 min	45 min	60 min
Optimal case	2UF-0LF-10B	4UF-0LF-10B	6UF-0LF-10B	2UF-0LF-10B	6UF-0LF-10B
Worst case	6UF-4LF-2B	6UF-4LF-4B	6UF-4LF-6B	6UF-4LF-2B	6UF-4LF-6B
Time-averaged difference – $\Delta TF_{o,w,avg}$ (°C)	1.94	1.91	1.55	3.49	2.18
End-value difference – $\Delta TF_{o,w,end}$ (°C)	1.82	1.78	1.51	3.28	1.99
Time-averaged difference – $\Delta TB_{o,w,avg}$ (°C)	2.51	2.44	1.89	4.09	2.36
End-value difference – $\Delta TB_{o,w,end}$ (°C)	2.78	2.76	2.22	5.28	2.98
Time-averaged difference – $\Delta TTS_{o,w,avg}$ (°C)	0.81	0.79	0.63	0.51	0.31
End-value difference – $\Delta TTS_{o,w,end}$ (°C)	0.60	0.59	0.48	0.30	0.18
Time-averaged difference – $\Delta TC_{o,w,avg}$ (°C)	0.70	0.68	0.54	0.64	0.49
End-value difference – $\Delta TC_{o,w,end}$ (°C)	0.40	0.39	0.32	0.60	0.46

consider individual differences such as gender and age, however, adjustments to the bioheat model would be needed as well as further experiments to validate the model.

Acknowledgements

This publication was made possible by NPRP grant# [NPRP 7 - 486 – 2 - 185] from the Qatar National Research Fund (a member of Qatar Foundation). The findings achieved herein are solely the responsibility of the authors.

Appendix A. Supplementary material

Supplementary data to this article can be found online at <https://doi.org/10.1016/j.applthermaleng.2018.09.057>.

References

[1] T. Kjellstrom, Impact of climate conditions on occupational health and related economic losses, Asia Pac. J. Publ. Health 28 (2016), <https://doi.org/10.1177/1010539514568711>.
 [2] H. Altinsoy, H.A. Yildirim, Labor productivity losses over western Turkey in the

- twenty-first century as a result of alteration in WBGT, *Int. J. Biometeorol.* 59 (2014) 463–471, <https://doi.org/10.1007/s00484-014-0863-z>.
- [3] D. Ouahrani, M. Itani, N. Ghaddar, K. Ghali, B. Khater, Experimental study on using PCMs of different melting temperatures in one cooling vest to reduce its weight and improve comfort, *Energy Build.* 155 (2017) 533–545.
 - [4] C. Gao, K. Kuklane, I. Holmér, Cooling vests with phase change materials: the effects of melting temperature on heat strain alleviation in an extremely hot environment, *Eur. J. Appl. Physiol.* 111 (2011) 1207–1216, <https://doi.org/10.1007/s00421-010-1748-4>.
 - [5] H. Hamdan, N. Ghaddar, D. Ouahrani, K. Ghali, M. Itani, PCM cooling vest for improving thermal comfort in hot environment, *Int. J. Therm. Sci.* 102 (2016) 154–167, <https://doi.org/10.1016/j.ijthermalsci.2015.12.001>.
 - [6] M. Itani, D. Ouahrani, N. Ghaddar, K. Ghali, W. Chakroun, The effect of PCM placement on torso cooling vest for an active human in hot environment, *Build. Environ.* 107 (2016) 29–42, <https://doi.org/10.1016/j.buildenv.2016.07.018>.
 - [7] H. Zhang, C. Huizenga, E. Arens, D. Wang, Thermal sensation and comfort in transient non-uniform thermal environments, *Eur. J. Appl. Physiol.* 92 (2004) 728–733, <https://doi.org/10.1007/s00421-004-1137-y>.
 - [8] J.D. Cotter, N.A.S. Taylor, The distribution of cutaneous sudomotor and alliesthesia thermosensitivity in mildly heat-stressed humans: an open-loop approach, *J. Physiol.* 565 (2005) 335–345, <https://doi.org/10.1113/jphysiol.2004.081562>.
 - [9] M. Nakamura, T. Yoda, L.I. Crawshaw, M. Kasuga, Y. Uchida, K. Tokizawa, K. Nagashima, K. Kanosue, Relative importance of different surface regions for thermal comfort in humans, *Eur. J. Appl. Physiol.* 113 (2013) 63–76.
 - [10] M. Nakamura, T. Yoda, L.I. Crawshaw, S. Yasuhara, Y. Saito, M. Kasuga, K. Nagashima, K. Kanosue, Regional differences in temperature sensation and thermal comfort in humans, *J. Appl. Physiol.* 105 (2008) 1897–1906.
 - [11] G.A. Selkirk, T.M. McLellan, Physical work limits for Toronto firefighters in warm environments, *J. Occup. Environ. Hyg.* 1 (2004) 199–212, <https://doi.org/10.1080/15459620490432114>.
 - [12] A.P. Chan, W. Yi, D.P. Wong, M.C. Yam, D.W. Chan, Determining an optimal recovery time for construction rebar workers after working to exhaustion in a hot and humid environment, *Build. Environ.* 58 (2012) 163–171, <https://doi.org/10.1016/j.buildenv.2012.07.006>.
 - [13] J.R. House, H.C. Lunt, R. Taylor, G. Milligan, J.A. Lyons, C.M. House, The impact of a phase-change cooling vest on heat strain and the effect of different cooling pack melting temperatures, *Eur. J. Appl. Physiol.* 113 (2012) 1223–1231, <https://doi.org/10.1007/s00421-012-2524-2>.
 - [14] C. Gao, K. Kuklane, F. Wang, I. Holmér, Personal cooling with phase change materials to improve thermal comfort from a heat wave perspective, *Indoor Air* 22 (2012) 523–530, <https://doi.org/10.1111/j.1600-0668.2012.00778.x>.
 - [15] M. Itani, N. Ghaddar, D. Ouahrani, K. Ghali, B. Khater, An optimal two-bout strategy with phase change material cooling vests to improve comfort in hot environment, *J. Therm. Biol.* 72 (2018) 10–25.
 - [16] J.C. Stevens, Variation of cold sensitivity over the body surface, *Sens. Processes* 3 (1979) 317–326 R.E..
 - [17] M. Itani, N. Ghaddar, K. Ghali, B. Khater, D. Ouahrani, W. Chakroun, Experimental study on effective placement of PCM packets in cooling vest to improve performance in warm environment, in: *Proceedings of the 2017 ASME Summer Heat Transfer Conference*, Paper Number: HT2017-4756, July 9–14, Bellevue, Washington, 2017.
 - [18] W. Karaki, N. Ghaddar, K. Ghali, K. Kuklane, I. Holmér, L. Vanggaard, Human thermal response with improved AVA modeling of the digits, *Int. J. Therm. Sci.* 67 (2013) 41–52, <https://doi.org/10.1016/j.ijthermalsci.2012.12.010>.
 - [19] M. Itani, N. Ghaddar, K. Ghali, D. Ouahrani, W. Chakroun, Cooling vest with optimized PCM arrangement targeting torso sensitive areas that trigger comfort when cooled for improving human comfort in hot conditions, *Energy Build.* 139 (2017) 417–425, <https://doi.org/10.1016/j.enbuild.2017.01.036>.
 - [20] N. McGinnis, Ergometry testing in the climatic chamber, *Sports Med.* 25 (1999) 86–89.
 - [21] ISO 7730, Ergonomics of the Thermal Environment-Analytical Determination and Interpretation of Thermal Comfort Using Calculation of the PMV and PPD Indices and Local Thermal Comfort Criteria, 2005.
 - [22] A.P. Avolio, Multi-branched model of the human arterial system, *Med. Biol. Eng. Compu.* 18 (1980) 709–718.
 - [23] W. Weng, X. Han, M. Fu, An extended multi-segmented human bioheat model for high temperature environments, *Int. J. Heat. Mass. Tran.* 75 (2014) 504–513, <https://doi.org/10.1016/j.ijheatmasstransfer.2014.03.091>.
 - [24] L.E. Dorman, G. Havenith, The effects of protective clothing on energy consumption during different activities, *Eur. J. Appl. Physiol.* 105 (2009) 463–470, <https://doi.org/10.1007/s00421-008-0924-2>.
 - [25] First Line Technology, Available at: <https://www.firstlinetech.com/product/swede-basic-cooling-vest/> (accessed 27 November 2017).
 - [26] A. Bejan, *Convection Heat Transfer*, second ed., Wiley-Interscience, 1994.
 - [27] K. Ghali, M. Othmani, B. Jreije, N. Ghaddar, Simplified heat transport model of a wind-permeable clothed cylinder subject to swinging motion, *Text. Res. J.* 79 (2009) 1043–1055.
 - [28] U. Danielsson, *Convection Coefficients in Clothing Air Layers*, PhD dissertation, The Royal Institute of Technology, Sweden, 1996.
 - [29] B.W. Jones, Y. Ogawa, Transient interaction between the human and the thermal environment, *ASHRAE Trans.* 98 (1993) 189–195.
 - [30] N.K. Dhand, M.S. Khatkar, Statulator: an online statistical calculator. Sample Size Calculator for Comparing Two Independent Proportions, 2014. <http://statulator.com/SampleSize/ss2PM.html> (accessed 7 March 2018).
 - [31] J. Pokorný, J. Fišer, M. Fojtín, B. Kopečková, R. Toma, J. Slabotínský, M. Jícha, Verification of Fiala-based human thermophysiological model and its application to protective clothing under high metabolic rates, *Build. Environ.* 126 (2017) 13–26.
 - [32] ASTM F1291-15, Standard Test Method for Measuring the Thermal Insulation of Clothing Using a Heated Manikin, ASTM International, West Conshohocken, PA, 2015.
 - [33] ASTM F2370-16, Standard Test Method for Measuring the Evaporative Resistance of Clothing Using a Sweating Manikin, ASTM International, West Conshohocken, PA, 2016.
 - [34] ISO, Hot environments, Estimation of heat stress on working man, based on the WBGT-index (wet bulb globe temperature) ISO 7243:1989. ISO Geneva, Switzerland, 1989.
 - [35] ISO 3801, Textiles-woven fabrics – determination of mass per unit length and mass per unit area, 1977.
 - [36] S.S. Pavlović, S.B. Stanković, D.M. Popović, G.B. Poparić, Transient thermal response of textile fabrics made of natural and regenerated cellulose fibers, *Polym. Test.* 34 (2014) 97–102.
 - [37] P. Lizák, S.C. Mojumdar, Thermal properties of textile fabrics, *J. Therm. Anal. Calorim.* 112 (2013) 1095–1100.
 - [38] G. Fu, A transient 3-D mathematical thermal model for the clothed human, PhD thesis, Kansas State University, 1995.
 - [39] E.A. McCullough, B.W. Jones, J. Huck, A comprehensive data base for estimating clothing insulation, *ASHRAE Trans.* 91 (1985) 29–47.
 - [40] E.A. McCullough, A data base for determining the evaporative resistance of clothing, *ASHRAE Trans.* 95 (1989) 316–328.
 - [41] ISO, Non-ducted Air Conditioners and Heat Pumps – Testing and Rating for Performance ISO 5151:2010(E), ISO Geneva, Switzerland, 2010.
 - [42] C. Chou, Y. Tochihara, T. Kim, Physiological and subjective responses to cooling devices on firefighting protective clothing, *Eur. J. Appl. Physiol.* 104 (2008) 369–374, <https://doi.org/10.1007/s00421-007-0665-7>.
 - [43] Y. Yang, A.P. Chan, Perceptual strain index for heat strain assessment in an experimental study: an application to construction workers, *J. Therm. Biol.* 48 (2015) 21–27, <https://doi.org/10.1016/j.jtherbio.2014.12.007>.
 - [44] ISO 9886: Ergonomics – evaluation of thermal strain by psychological measurements, 2008.
 - [45] ISO 12894 (E): Ergonomics of the thermal environment – Medical supervision of individuals exposed to extreme hot or cold environment, 2008.
 - [46] W.D. Vanmarckenlichtentbelt, H.A. Daanen, L. Wouters, R. Fronczek, R.J. Raymann, N.M. Severens, et al., Evaluation of wireless determination of skin temperature using iButtons, *Physiol. Behav.* 88 (2006) 489–497, <https://doi.org/10.1016/j.physbeh.2006.04.026>.
 - [47] M. Nakayoshi, M. Kanda, R. Shi, R.D. Dear, Outdoor thermal physiology along human pathways: a study using a wearable measurement system, *Int. J. Biometeorol.* 59 (2014) 503–515, <https://doi.org/10.1007/s00484-014-0864-y>.
 - [48] A.C. Guyton, J.E. Hall, *Textbook of medical physiology*, Saunders, Philadelphia, PA, 1996.
 - [49] F.H. Netter, *Atlas of human anatomy*, second ed., Novartis, East Hanover, 1997.
 - [50] B. Haugan, A.K. Langerud, H. Kalvøy, K.F. Frøslie, E. Riise, H. Kapstad, Can we trust the new generation of infrared tympanic thermometers in clinical practice? *J. Clin. Nurs.* (2012), <https://doi.org/10.1111/j.1365-2702.2012.04077.x>.
 - [51] M. Chudecka, A. Lubkowska, Thermal imaging of body surface temperature distribution in women with anorexia nervosa, *Eur. Eat. Disord. Rev.* 24 (2016) 57–61.
 - [52] N.L. Ramanathan, A new weighting system for mean surface temperature of the human body, *J. Appl. Physiol.* 19 (1964) 531–533.
 - [53] T. Langø, R. Nesbakken, H. Færevik, K. Holbo, J. Reitan, Y. Yavuz, et al., Cooling vest for improving surgeons' thermal comfort: a multidisciplinary design project, *Minim. Invasive Ther. Allied Technol.* 18 (2009) 20–29, <https://doi.org/10.1080/13645700802649383>.
 - [54] W. Liu, Z. Lian, Q. Deng, Y. Liu, Evaluation of calculation methods of mean skin temperature for use in thermal comfort study, *Build. Environ.* 46 (2011) 478–488, <https://doi.org/10.1016/j.buildenv.2010.08.011>.
 - [55] R. Ilmarinen, H. Lindholm, K. Koivistoinen, P. Helistö, Physiological evaluation of chemical protective suit systems (CPSS) in hot conditions, *Int. J. Occup. Saf. Ergon.* 10 (2004) 215–226, <https://doi.org/10.1080/10803548.2004.11076609>.
 - [56] M. Gallagher, R.J. Robertson, E.F. Nagle, F.L. Goss, M.A. Schafer, D. Hostler, et al., Development of a perceptual hyperthermia index to evaluate heat strain during treadmill exercise, *Med. Sci. Sports Exerc.* 42 (2010) 670–671, <https://doi.org/10.1249/01.mss.0000385870.76923.50>.
 - [57] R. Nielsen, D.C.E. Gavhed, H. Nilsson, Thermal function of a clothing ensemble during work: dependency on inner clothing layer fit, *Ergonomics* 32 (1989) 1581–1594, <https://doi.org/10.1080/00140138908966927>.
 - [58] J. Webster, E. Holland, G. Sleivert, R. Laing, B. Niven, A light-weight cooling vest enhances performance of athletes in the heat, *Ergonomics* 48 (2005) 821–837, <https://doi.org/10.1080/00140130500122276>.
 - [59] H. Wang, S. Hu, Experimental study on thermal sensation of people in moderate activities, *Build. Environ.* 100 (2016) 127–134, <https://doi.org/10.1016/j.buildenv.2016.02.016>.
 - [60] J. Cohen, *Statistical Power Analysis for the Behavioral Sciences*, second ed., L. Erlbaum Associates, Hillsdale, NJ, 1988.
 - [61] J.W. Choi, M.J. Kim, J.Y. Lee, Alleviation of heat strain by cooling different body areas during red pepper harvest work at WBGT 33 °C, *Ind. Health* 46 (2008) 620–628, <https://doi.org/10.2486/indhealth.46.620>.

- [62] M. Nakahashi, M. Murayama, H. Monobe, H. Ikuno, Relationship between wearing time period and moving quantity of fireman's turnouts based on a scenario of fire, *Jpn. J. Physiol. Anthropol.* 8 (2003) 83–89.
- [63] M. Jetté, K. Sidney, G. Blümchen, Metabolic equivalents (METS) in exercise testing, exercise prescription, and evaluation of functional capacity, *Clin. Cardiol.* 13 (1990) 555–565, <https://doi.org/10.1002/clc.4960130809>.
- [64] G.P. Bates, J. Schneider, Hydration status and physiological workload of UAE construction workers: a prospective longitudinal observational study, *J. Occup. Med. Toxicol.* 3 (2008) 21, <https://doi.org/10.1186/1745-6673-3-21>.
- [65] V.S. Miller, G.P. Bates, The thermal work limit is a simple reliable heat index for the protection of workers in thermally stressful environments, *Ann. Occup. Hyg.* 51 (2007) 553–561, <https://doi.org/10.1093/annhyg/mem035>.